nks

Nordisk kernesikkerhedsforskning
Norrænar kjarnöryggisrannsóknir
Pohjoismainen ydinturvallisuustutkimus
Nordisk kjernesikkerhetsforskning
Nordisk kärnsäkerhetsforskning
Nordic nuclear safety research

NKS-73
ISBN 87-7893-129-0

Structural integrity of a reinforced concrete structure and a pipe outlet under hydrogen detonation conditions

Arja Saarenheimo, Ari Silde & Kim Calonius
VTT Industrial Systems, Finland

May 2002

Abstract

Structural integrity of a reinforced concrete wall and a pipe penetration under detonation conditions in a selected reactor building room of Olkiluoto BWR were studied. Hydrogen leakage from the pressurised containment to the surrounding reactor building is possible during a severe accident. Leaked hydrogen tends to accumulate in the reactor building rooms where the leak is located leading to a stable stratification and locally very high hydrogen concentration. If ignited, a possibility to flame acceleration and detonation cannot be ruled out.

The structure may survive the peak detonation transient because the eigenperiod of the structure is considerably longer than the duration of the peak detonation. However, the relatively slowly decreasing static type pressure after a peak detonation damages the wall more severely. Elastic deformations in reinforcement are recoverable and cracks in these areas will close after the pressure decrease. But there will be remarkable compression crushing and the static type slowly decreasing over pressure clearly exceeds the loading capacity of the wall.

Structural integrity of a pipe outlet was considered also under detonation conditions. The effect of drag forces was taken into account. Damping and strain rate dependence of yield strength were not taken into consideration. The boundary condition at the end of the pipe line model was varied in order to find out the effect of the stiffness of the pipeline outside the calculation model. The calculation model where the lower pipe end is free to move axially, is conservative from the pipe penetration integrity point of view. Even in this conservative study, the highest peak value for the maximum plastic deformation is 3.5%. This is well below the success criteria found in literature.

Key words

Non-linear reinforced concrete, pipe outlet, hydrogen detonation, finite element analysis

NKS-73
ISBN 87-7893-129-0

The report can be obtained from
NKS Secretariat
P.O. Box 30
DK – 4000 Roskilde
Denmark

Phone +45 4677 4045
Fax +45 4677 4046
www.nks.org
e-mail nks@catscience.dk

Structural integrity of a reinforced concrete structure and a pipe outlet under hydrogen detonation conditions

Arja Saarenheimo, Ari Silde, Kim Calonius

Acknowledgements

This report is a part of STIN (Structural Integrity) project in FINNUS, the Finnish Research Programme on Nuclear Power Plant Safety. This study is funded by Nordic Nuclear Safety Research (NKS) SOS-2 project and by Ministry of Trade and Industry (KTM). The authors are indepted to Mr. Heikki Sjövall, Mr. Timo Kukkola and Mr. Paulus Smeekes from Teollisuuden Voima Ltd (TVO) for their technical support and review of the report.

Espoo

Authors

Table of contents

1 Introduction

Large amount of hydrogen may release into a BWR containment during severe accidents. Due to the thermal and pressure loads the containment is exposed to, hydrogen leakage from the containment into surrounding reactor building rooms cannot be totally excluded. Hydrogen may accumulate in the reactor building and, in the presence of normal air, form flammable and even detonable mixtures leading to pressure loads on pipes and walls. Particular interest is whether the containment integrity can be jeopardised by an external detonation. In particular, a damage of pipe penetrations may lead to an early release of fission products from the containment.

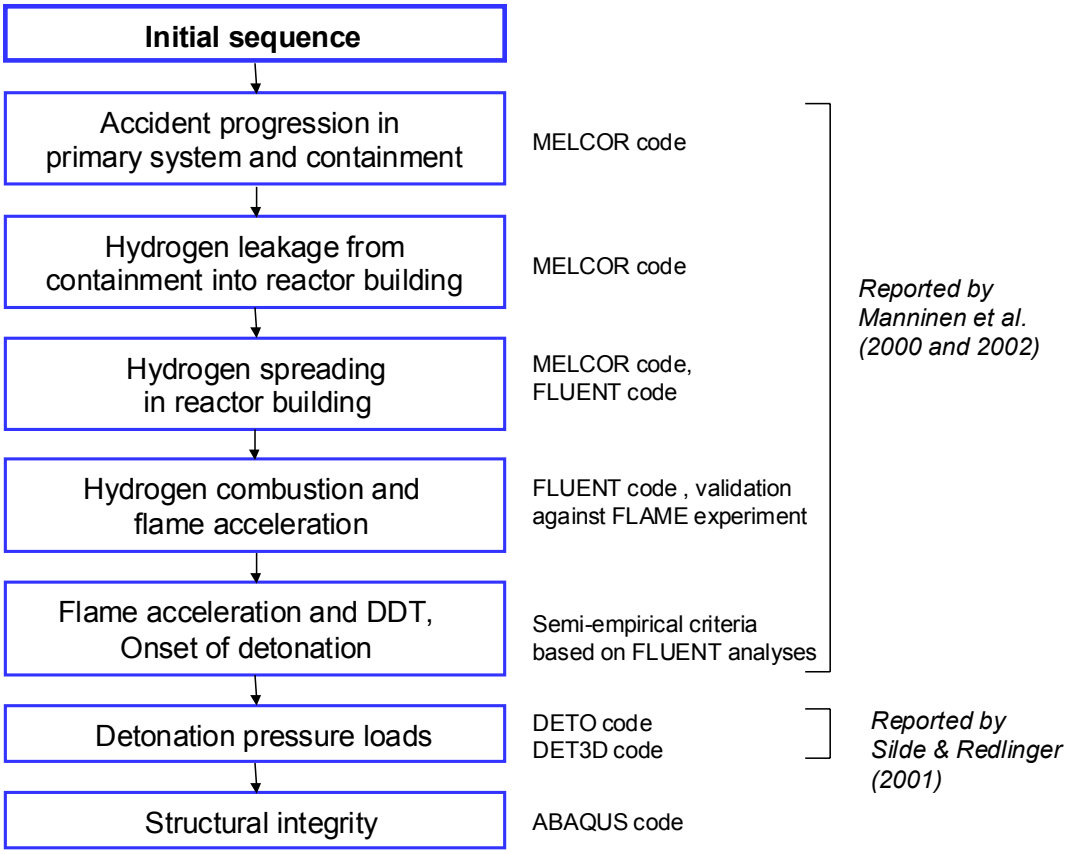

Figure 1. Stages of research of hydrogen behaviour in Olkiluoto reactor building.

Quite extensive studies were carried out in order to predict the pressure transients for structural analyses. This work is reported by Manninen et al. (2000 and 2002) and Silde & Redlinger (2001) (Fig. 1). Some preliminary studies concerning the hydrogen issue in Olkiluoto BWR reactor building were also performed by Silde & Lindholm (2000) and Saarenheimo (2000). Conclusion of these studies was that hydrogen accumulates in the reactor building rooms leading to a stable stratification and locally very high hydrogen concentration. If ignited, a possibility to flame acceleration and detonation cannot be ruled out.

This paper concentrates on three-dimensional detonation simulations and structural integrity analyses in one selected room of Olkiluoto BWR reactor building (last two steps in Fig. 1). Detonation simulations were carried out with the DET3D code developed at Forschungszentrum Karlsruhe (FzK). A data transfer tool was developed to enable a flexible data transfer between the DET3D and the ABAQUS codes (Silde & Pättikangas, 2001). Non-linear finite element analyses of the reinforced concrete structure were carried out by the ABAQUS/Explicit program using the pressure loads obtained from the DET3D simulations as input. The reinforcement and its non-linear material behaviour as well as the tensile cracking of concrete were modelled. An overview

of the whole analysis chain, main results of the DET3D analyses and some preliminary results of structural analyses are presented in this paper.

2 Numerical simulation of loading transient

The investigated accident scenario is a station blackout resulting in a loss of the reactor building ventilation. A conservative assumption of 100% zirconium oxidation in a core was made leading to 1900 kg hydrogen generation within the containment. The considered reactor building room is adjacent to the containment wall and has a total volume of 856 m^3 (Fig. 2). The room is about 33 m tall, but very narrow (Fig. 3). The hydrogen leakage is assumed to occur in the penetration inlet at an elevation of 5 m below the room ceiling (at level around +26 m). The leak area was assumed to be 20 mm^2, which corresponds to around 10 times the nominal leakage of the containment.

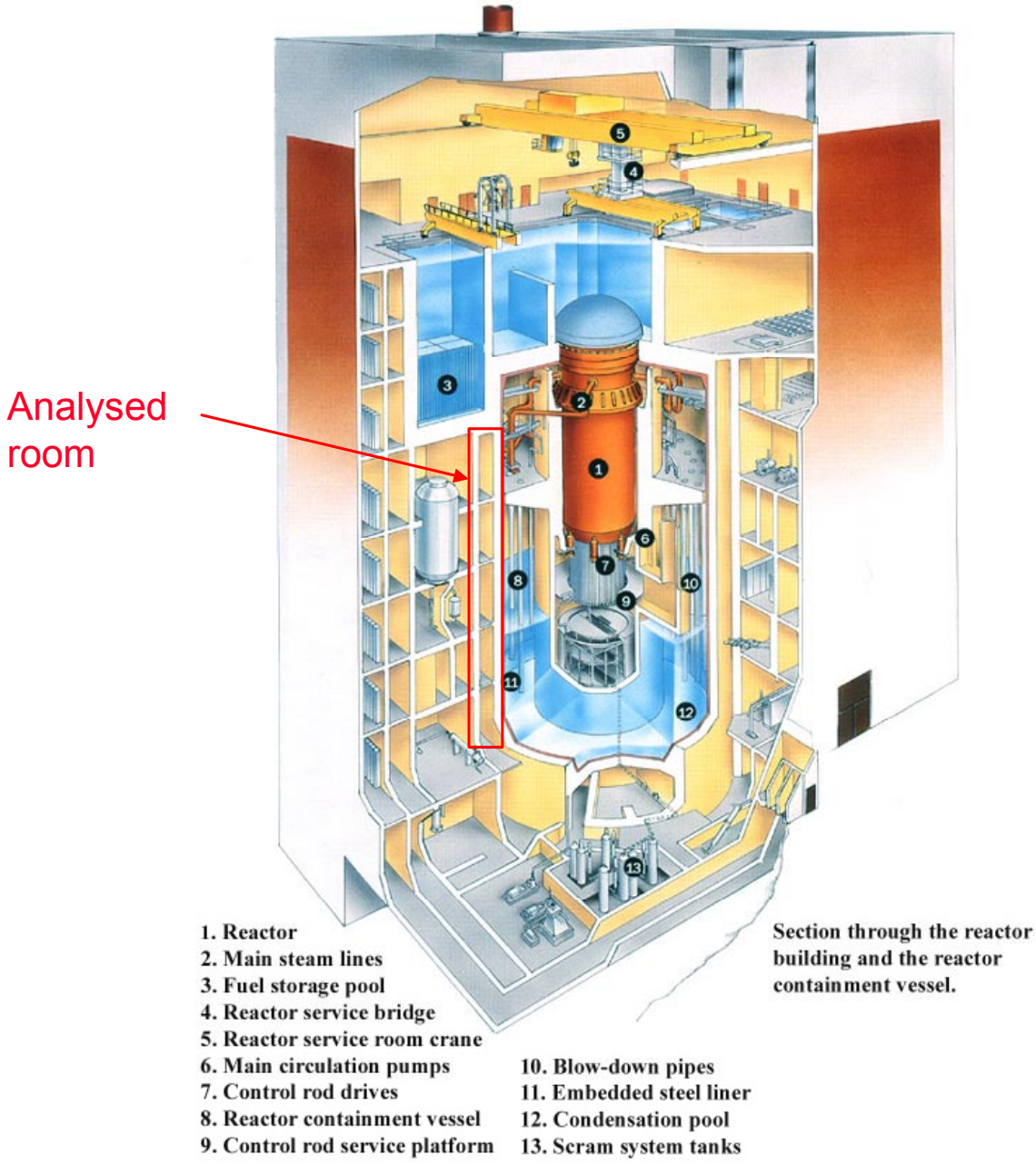

Figure 2. Olkiluoto BWR containment and the adjacent reactor building rooms.

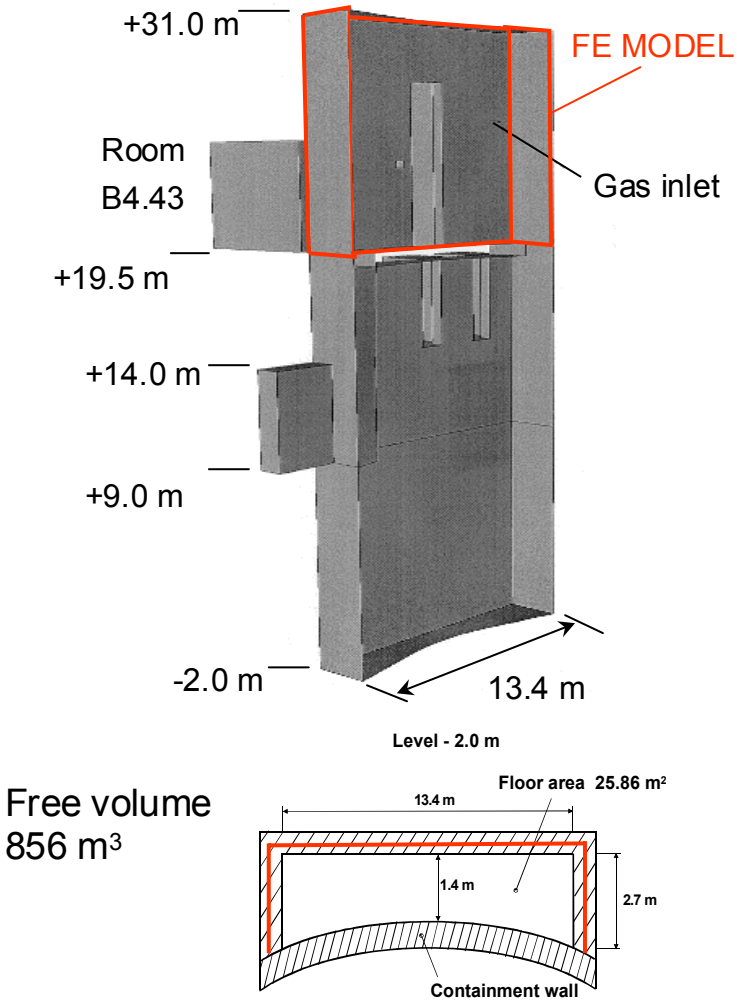

Figure 3. Geometry of analysed reactor building room B.60.80.

2.1 Results of DET3D simulation

The model of the detonation simulation used an uniform cartesian grid consisting of about 778 000 cells corresponding to the cell size of 0.117 m. All concrete boundaries of the room were modelled. Two pipelines were also included in the model. These pipelines leave horizontally from the containment wall at level + 26 m, make a 90-degree angle and continue vertically to the bottom of the room. Both pipelines were constructed of rectangular form in the model. This simplification does not reduce significantly the accuracy of the simulation. All other internal obstacles were ignored. This is justified by the fact that the upper part of the room, where the hydrogen existed, is relatively open space. Influence of obstacles in very fast detonation processes can be considered insignificant.

The initial gas concentrations relied to earlier CFD simulation with the FLUENT code (Manninen et al., 2000). Prior to beginning of detonation, about 3.5 kg hydrogen was assumed to release into the reactor building room. At that time, very high concentration gradient exists in the room (Fig. 4). The gas composition in the upper part of the room is nearly stoichiometric while no hydrogen exists near the floor elevation. Same values for the initial pressure (0.1065 MPa), temperature (301.2 K) and density (0.9 kg m^{-3}) were used throughout the computational grid. The detonation was ignited at an elevation of 2.5 m below the ceiling (level + 28.5 m) where there is a fluorescent lamp. The ignition occurred in the middle of the narrow end wall of the room. The detonation was initiated by introducing a very high pressure (6 MPa) and temperature (4000 K) into a desired ignition location in the computational grid.

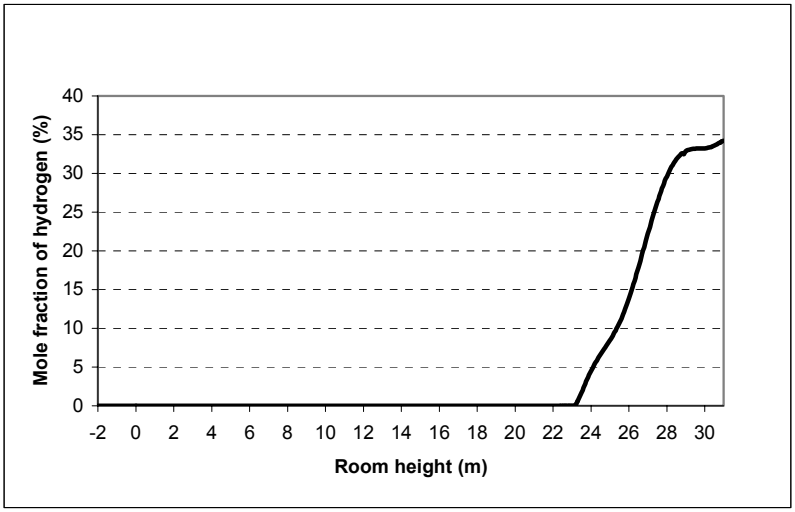

Figure 4. Initial profile of the mole fraction of hydrogen in analysed reactor building room.

Three–dimensional detonation simulation was carried out with a finite difference code DET3D developed at Forschungszentrun Karlsruhe (FzK) (Breitung and Redlinger, 1994). The approach of the code enables the detailed assessment of detonation processes and consequential pressure loads in a real 3D geometry taking into account the multiple reflections and interactions of the shock waves.

Detailed description of the DET3D results can be found in reference (Silde & Redlinger, 2001, simulation Case 2). As seen in Figure 4, the detonable gas mixture is located above the level around + 26 m in the room. The mole fraction of hydrogen above the gas inlet (level + 28 m) is roughly 30 – 34 % and the mole fraction of oxygen about 12 - 13%.

Propagation of shock waves after the ignition of detonation can be seen in Figure 5, where the pressure contours at four selected instants of time are illustrated. A spherically expanding detonation wave is formed propagating throughout the upper part of the room. The detonation reaches the room ceiling at $t \approx 1$ ms, the left-hand side pipe penetration at about $t = 2$ ms, the internal concrete wall in the middle of the upper part of the room at $t \approx 3$ ms and the end wall opposite the ignition location at $t \approx 6.5$ ms. The detonation wave cannot propagate below the level around + 26 m, where a lean hydrogen mixture exists. However, detonation-induced decaying shock waves propagate downwards throughout the whole room reaching the bottom of the room roughly at $t \approx 45$ ms.

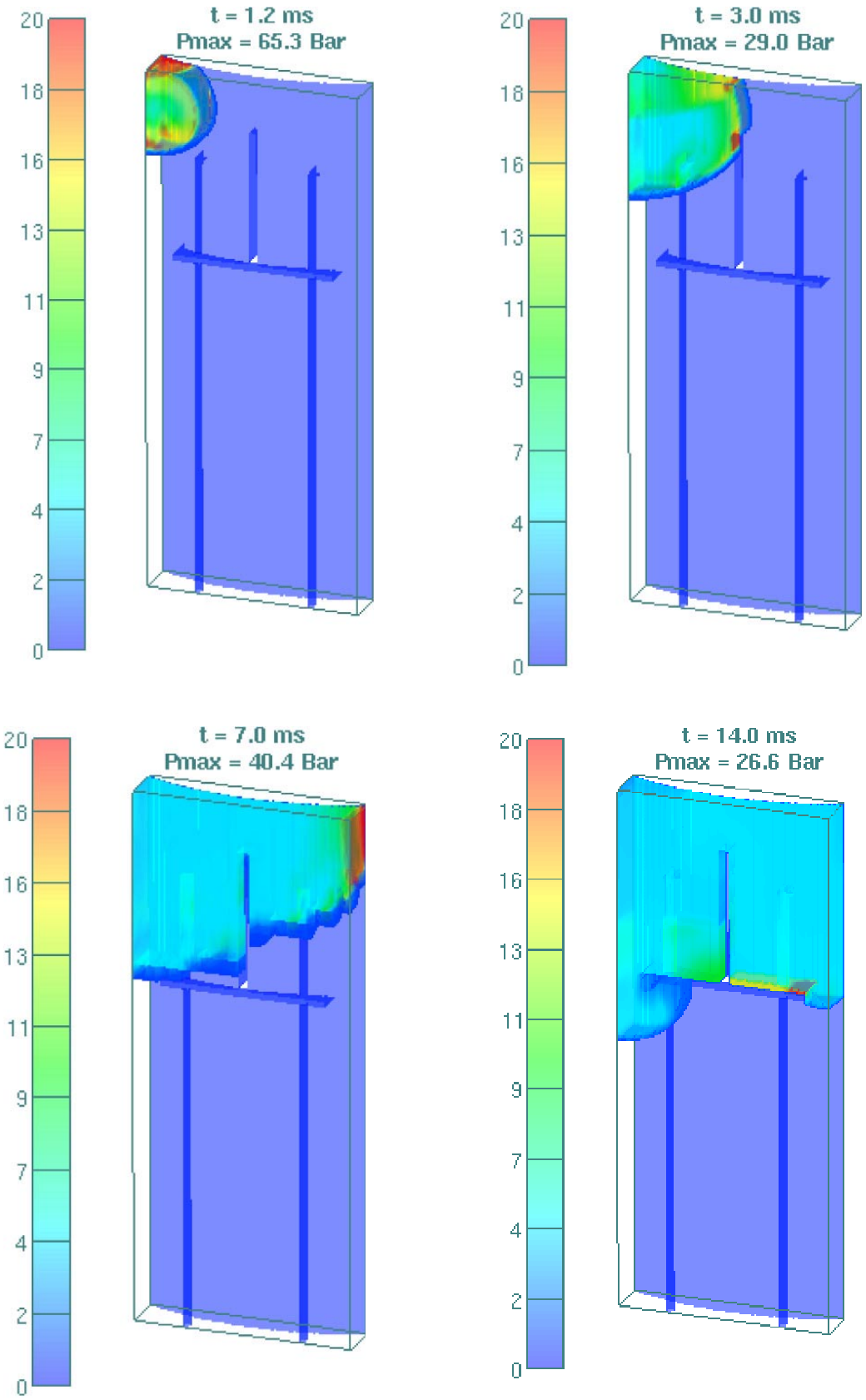

Figure 5. Contours of pressure at four selected instants of time.

The maximum pressure value found in each computational cell during the 150 ms simulation is illustrated in Fig. 6. The highest pressure peak of about 7.0 MPa is observed in the upper corner of the room beside the containment wall (level + 31 m). History of simulated pressures on the reinforced concrete wall at two different elevations of the room is illustrated in Figure 7. The pressure history near the room boundaries is characterised by a high and short (order of few milliseconds) pressure transient caused by shock reflection. After the first spike, the pressure decreases relatively slowly. The pressure fluctuation after the first spike is caused by the later interactions of shock waves and their reflections from the walls. Because the detonation cannot propagate to the bottom of the room, the highest pressure value there is only about 0.8 MPa due to reflections of decaying shock waves.

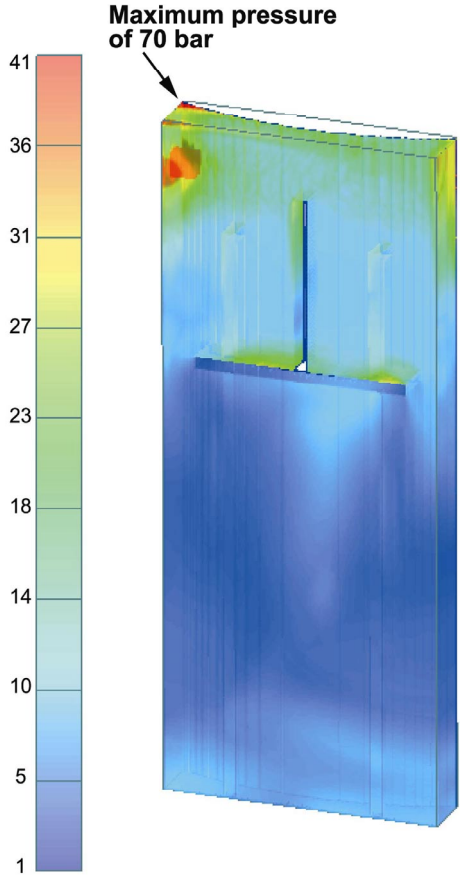

Figure 6. Contours of maximum pressure (bar) value found in each cell during the 150 ms simulation.

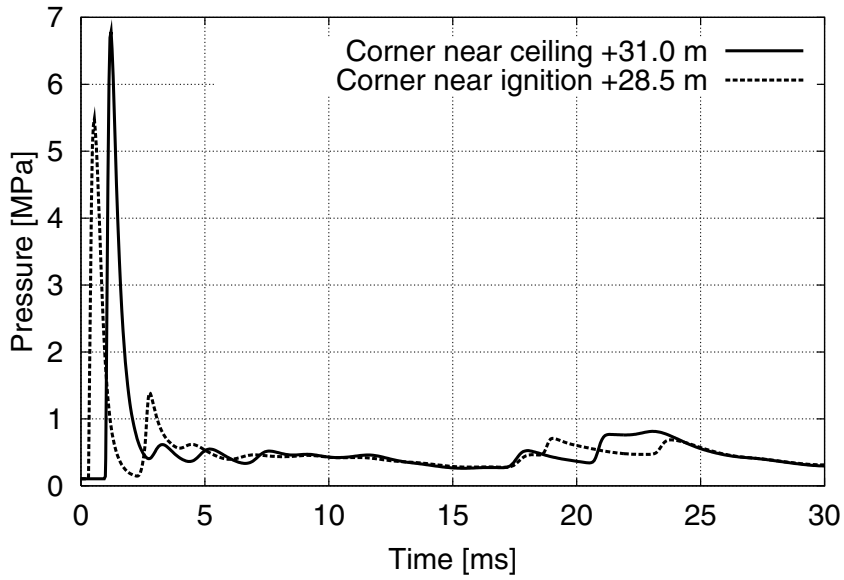

Figure 7. Simulated reflection pressures at two different elevations of the room.

Normalised pressure impulses to a reinforced concrete wall structure at three different elevations during a 30 ms simulation are shown in Figure 8. Comparison to Fig. 7 indicates that the pressure spikes from the first shock reflections result in the impulse loads less than 5 kPa-s. Later on, the increase of impulses is caused by relatively slowly decreasing pressure after the first spike and the later reflections of the shock waves. The highest pressure impulses on the wall structure during the 30 ms simulation are around 13 kPa-s.

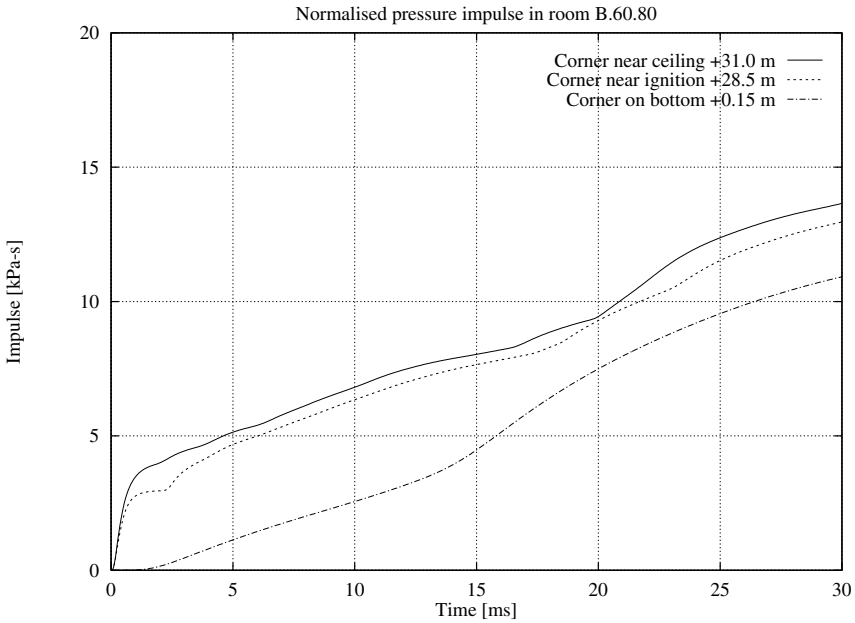

Figure 8. Normalised pressure impulses at three different elevations.

Simulated pressure values around the pipe penetration (near ignition location) and around the pipeline at five different elevations are illustrated in Figures 9-14. The legend of the figures shows the (x,y,z)-coordinate, where the pressure is plotted. Maximum pressure value around the pipe penetration beside the containment wall is approximately 1.8 MPa at $t \approx 2$ ms (Fig. 9). After this instant of time, the pressure remains below 1.0 MPa. The maximum pressure value on the vertical pipeline is approximately 1.5 MPa above the level around + 24 m (Figs 10 and 11). Below this elevation, the pressure spikes are lower because the detonable gas mixture exists only above the level + 26 m (Figs 12 and 13). In the lower elevation at + 19.64 m, relatively high pressure spike

(≈ 2 MPa) is observed (Fig. 14). This is caused by the reflection of shock waves from the internal concrete floor at level + 19.5 m.

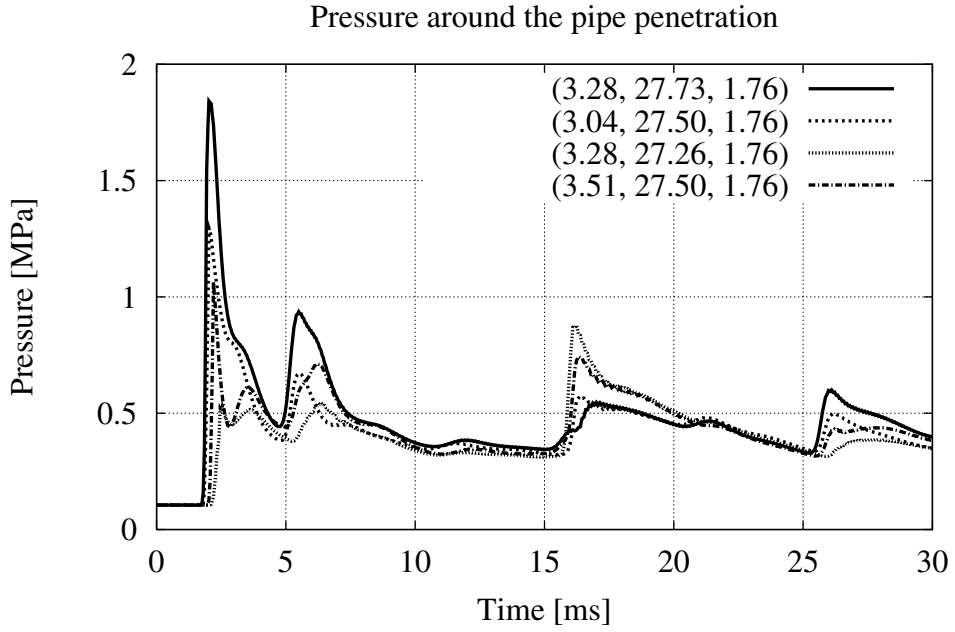

Figure 9. Pressure around the pipe penetration.

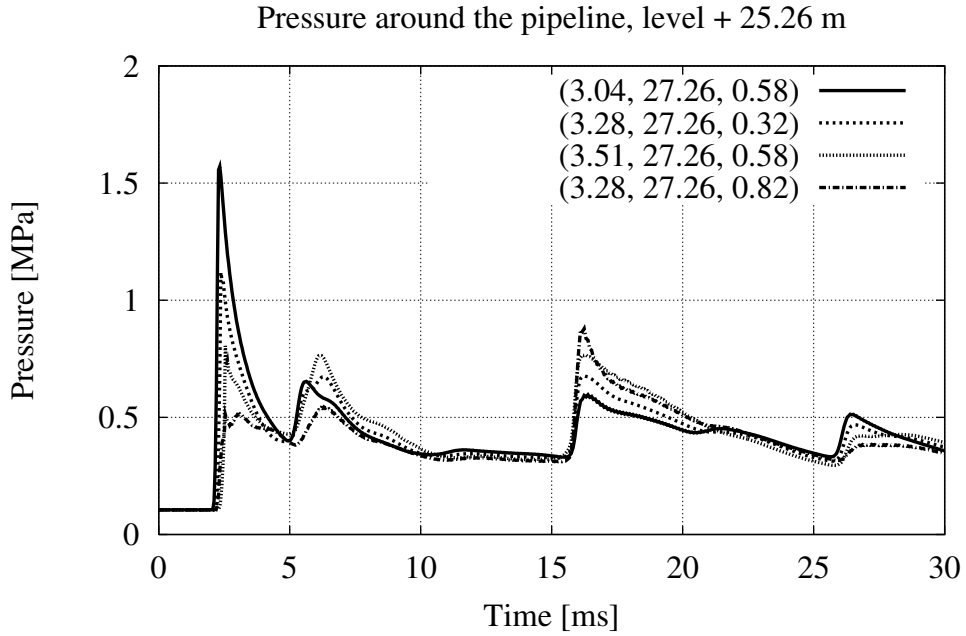

Figure 10. Pressure around the vertical pipeline at level + 25.26 m.

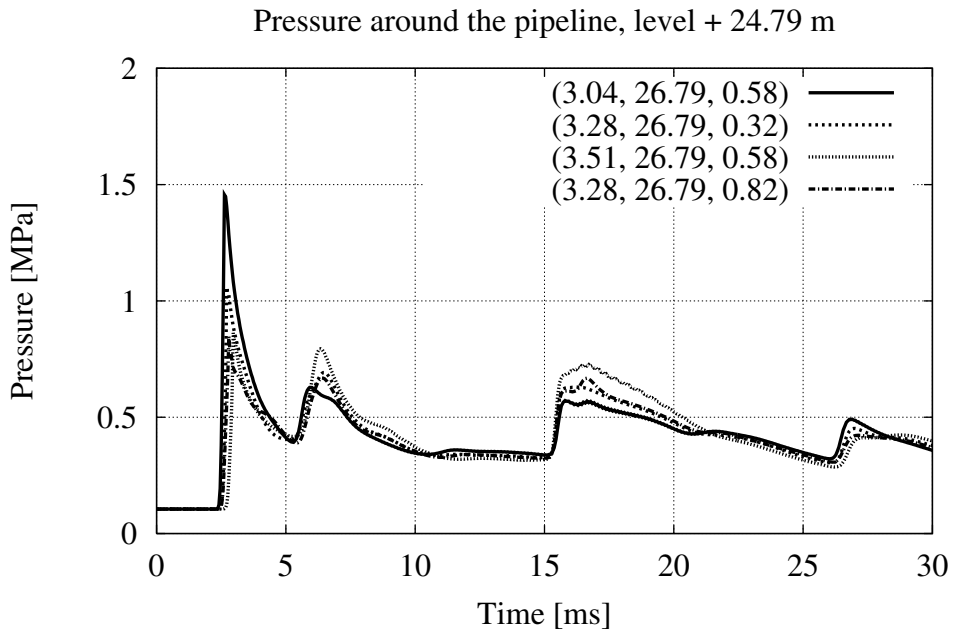

Figure 11. Pressure around the vertical pipeline at level + 24.79 m.

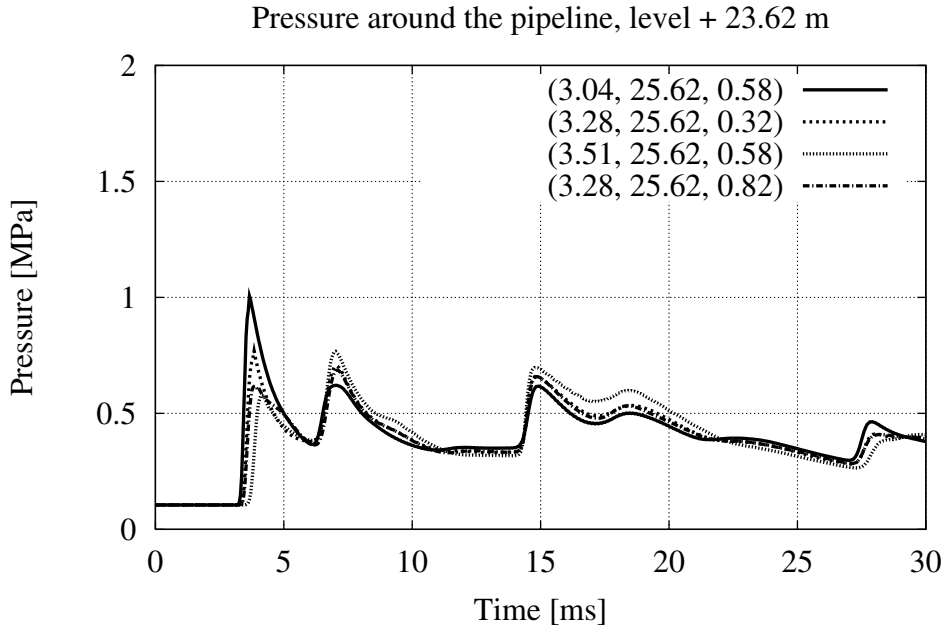

Figure 12. Pressure around the vertical pipeline at level + 23.62 m.

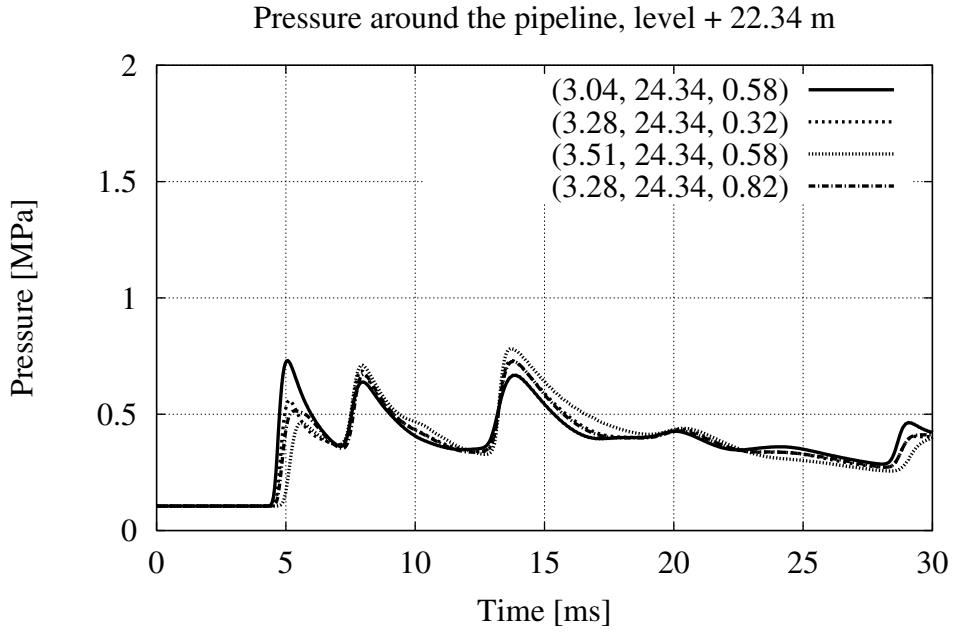

Figure 13. Pressure around the vertical pipeline at level + 22.34 m.

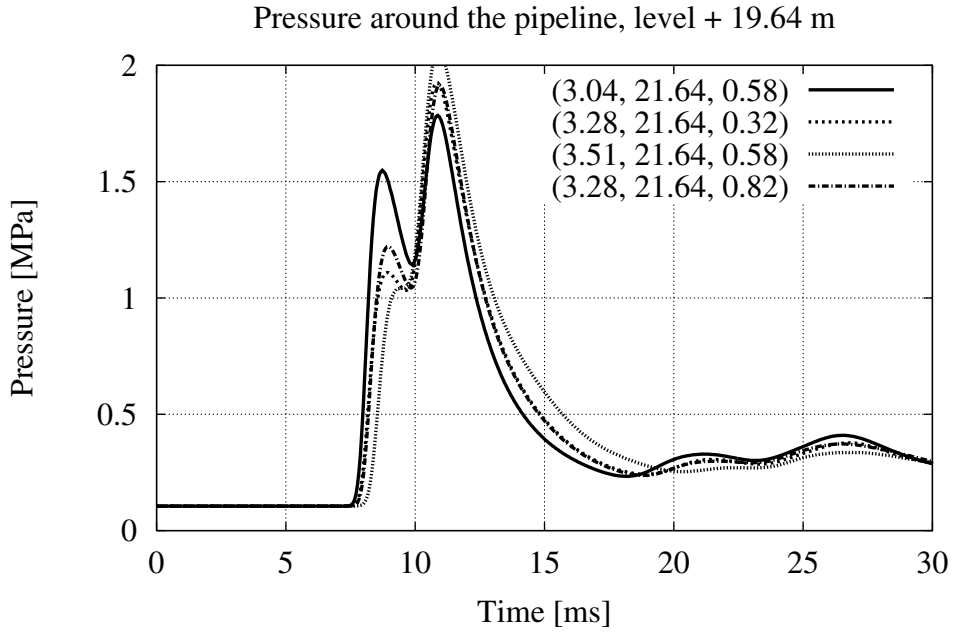

Figure 14. Pressure around the vertical pipeline at level + 19.64 m

2.2 Drag Forces to Internal Pipeline

Detonation pressure as modelled by DET3D defines the thermodynamic state of the fluid representing so called "local" properties of the fluid. Any directed motion as associated with stream velocity is, therefore, considered irrelevant.

However, if a structure like a pipe line is affected by a moving stream, it renders the stream stagnant and the molecular collisions induce excess forces on a structure. These forces are quite analogous to those developed by natural wind (Kinney & Graham, 1985). The wind forces are most conveniently studied by methods developed for the inverse problem: the drag forces on moving bodies. Data on drag forces can be represented as a dimensionless drag coefficient C_d.

Assuming that the average density of gas is not affected by the presence of structure, the average pressure drop p_d that accounts for the drag force per unit of projected area can be expressed as

$$p_d = \frac{1}{2} C_d \rho u^2 \tag{1}$$

where ρ is the average gas density and u is the average stream velocity.

As seen in Equation (1) the drag force is proportional to square of stream velocity. The drag coefficient is dependent on the geometry of object and the experimental values can be found in literature for various structure shapes.

In this study, the DET3D simulation indicated that the local gas velocities during the detonation were very high (up to 1000 m/s) in certain parts of the reactor building room. With respect to integrity of the internal pipeline and the pipe penetration, the drag forces must be, therefore, taken into account.

The effect of drag forces on the pipeline and connected valve in Olkiluoto reactor building room B.60.80 was approximately estimated using the following method. The average gas densities and velocities around the pipeline as a function of time were defined from the DET3D simulation. A value of 1.2 was used as the drag coefficient C_d for the pipeline of cylindrical shape (Kinney & Graham, 1985, Table VIII). The excess pressure drop across the pipeline caused by the drag was evaluated according to Equation (1). Total pressure drop across the pipe was assumed to be a sum of the "local" pressure differences predicted by DET3D (chapter 2.1) and the drag pressure drops estimated according to Equation 1.

It should be mentioned that the drag forces on the pipeline were defined using a very rough method. Drag values for all computational cells around the pipeline were not specified. Instead of that, only some selected representative points were selected, each of which covered the certain surface area of the pipeline.

Typical pressure drops around the pipeline caused by the drag forces are shown in Figs. 15-22. Direction of drag forces are extrapolated according to Fig. 33. Positive x-direction corresponds to 1-direction in the coordinate system of Fig. 33. Y-direction corresponds to negative 2-direction in Fig. 33.

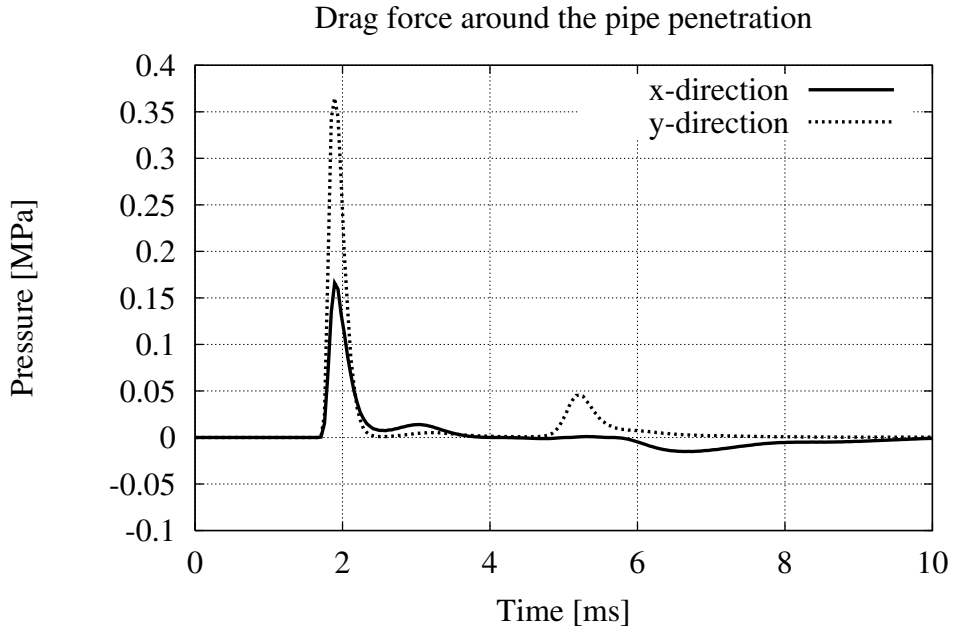

Figure 15. Drag force around the pipe penetration beside the containment wall.

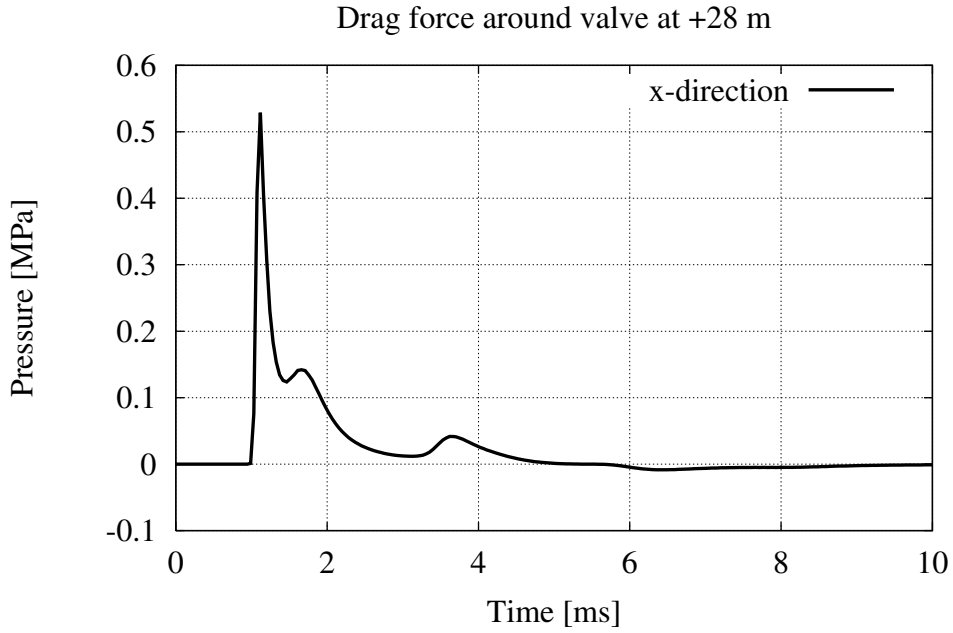

Figure 16. Drag force on the top of the valve system at level + 28.0 m.

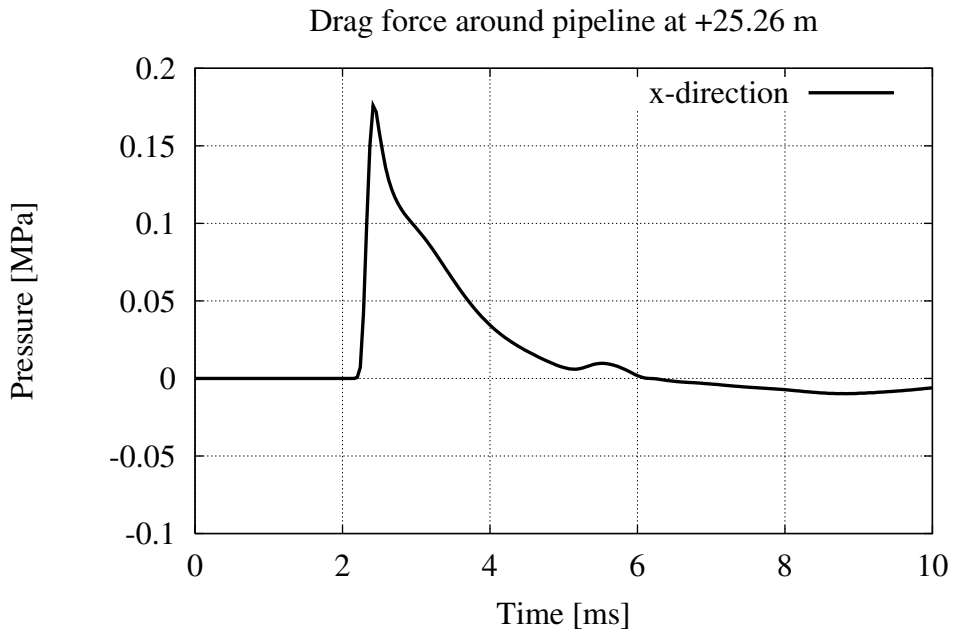

Figure 17. Drag force around the vertical pipeline at level +25.26 m.

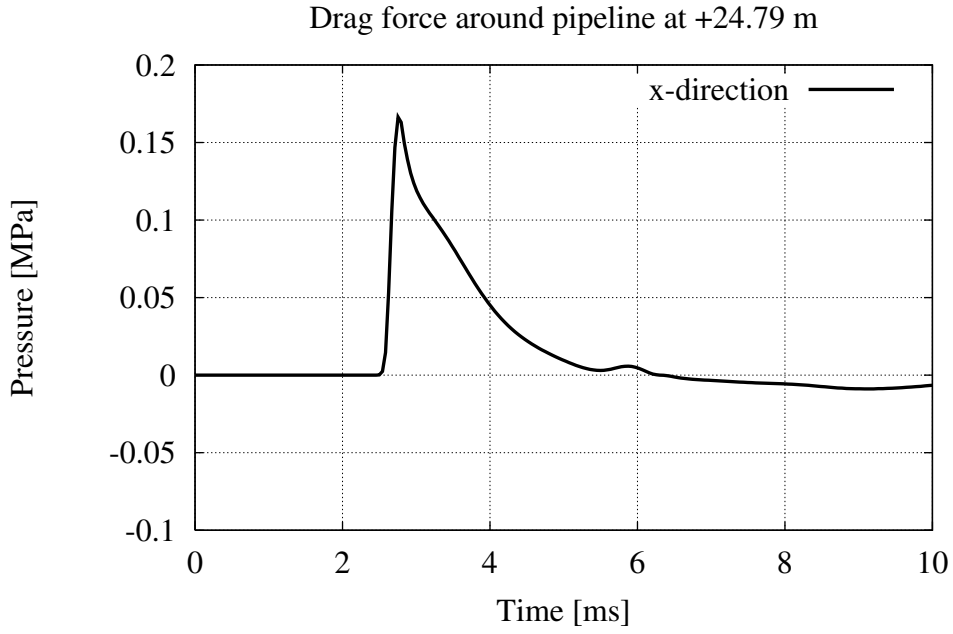

Figure 18. Drag force around the vertical pipeline at level +24.79 m.

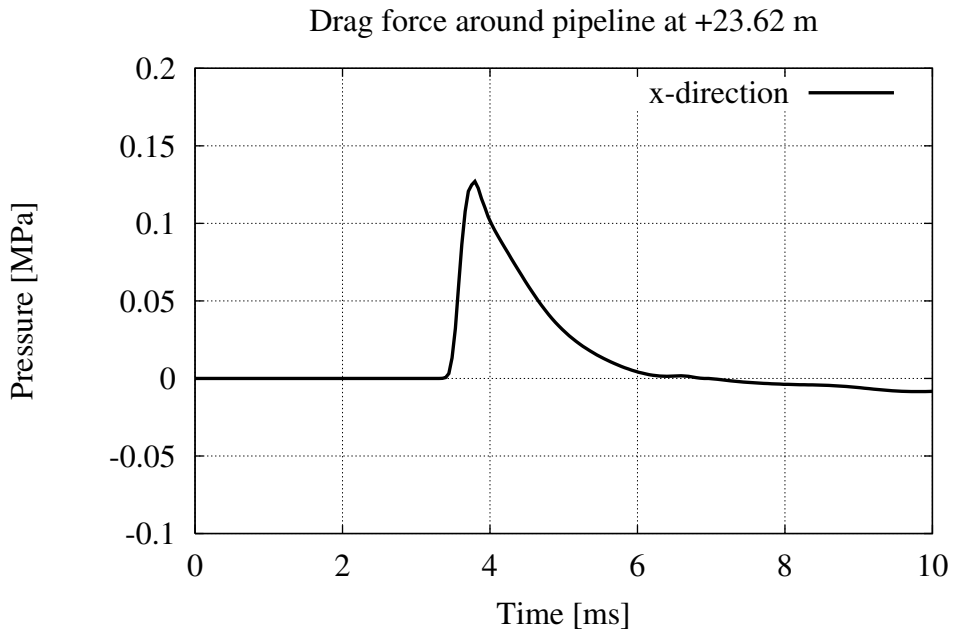

Figure 19. Drag force around the vertical pipeline at level +23.62 m.

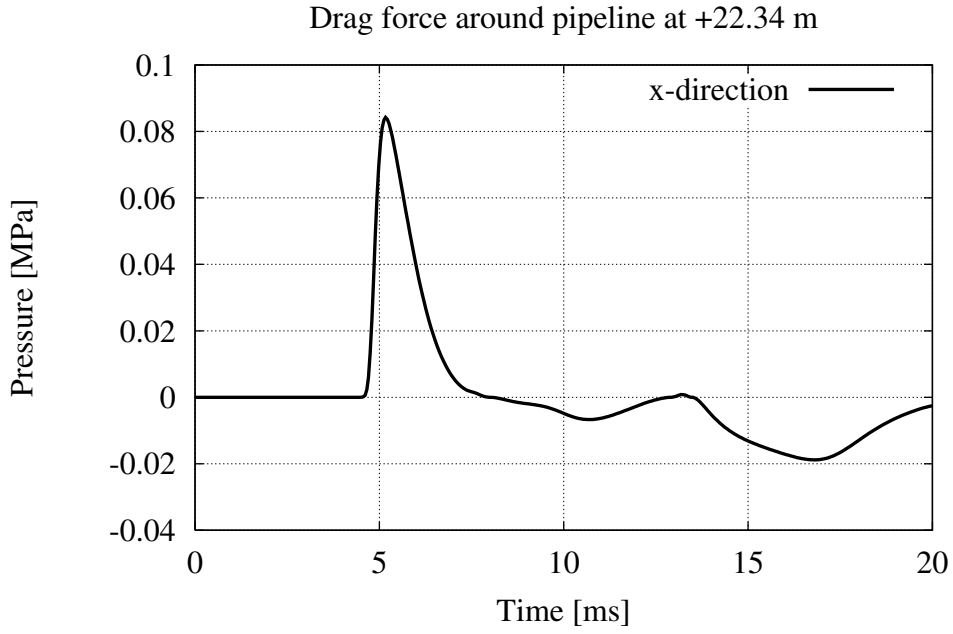

Figure 20. Drag force around the vertical pipeline at level +22.34 m.

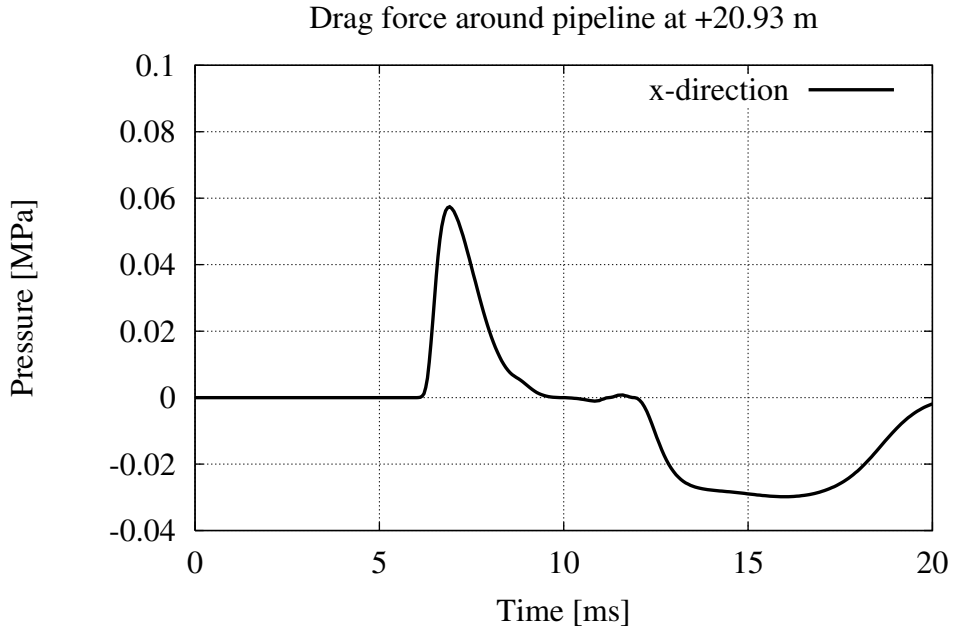

Figure 21. Drag force around the vertical pipeline at level +20.93 m.

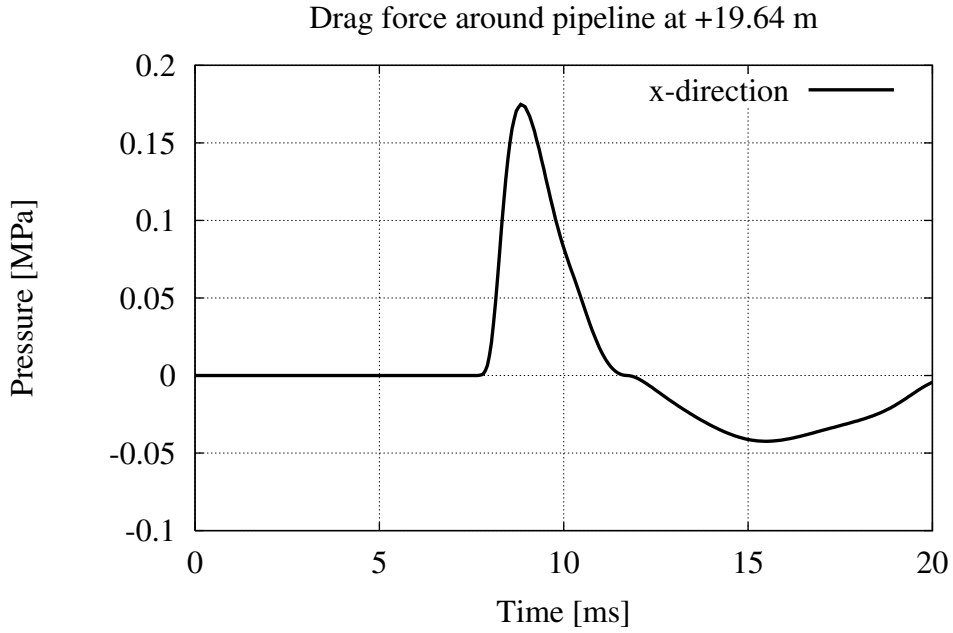

Figure 22. Drag force around the vertical pipeline at level +19.64 m.

Strongest sideward (x-direction) drag force was about 0.5 MPa and was exerted to the upper part of the isolation valve at level + 28 m (Fig. 16). At that elevation, the expanding detonation wave impacted directly the valve system. Because the detonation wave cannot propagate below the level around + 26 m, the drag forces around the pipeline are smaller below this elevation (Figs 17-22).

Vertical drag force (from top to bottom) is maximally about 0.35 MPa effecting on the horizontal part of the pipeline at level around + 25.5 m (Fig. 15, y-direction).

The drag force at level + 19.64 m (Fig. 22) is slightly strengthened by the reflections of shock waves from the internal concrete wall at level + 19.5 m (compare to Fig. 21).

3 Structural analyses

3.1 Reinforced concrete structure

Dynamic non-linear analyses of this reinforced concrete structure were carried out by ABAQUS/Explicit program (ABAQUS Theory Manual 1998), which is based upon the implementation of an explicit integration rule together with the use of diagonal element mass matrices. The equations of motion are integrated using the explicit central difference integration rule. Because peak pressure transients mainly occurred in the upper part of room B60.80, only the upper parts of the walls and pipeline were considered in the structural analyses. The part of the structure modelled by finite elements (FE) is indicated in Fig. 3 by red colour. Pressure loads are obtained from detonation simulation analyses reported in chapter 2. Pressure spikes during the first 30 ms were assumed as loading and after that the overpressure was assumed to decrease to zero during 0.25 s, because the room contains pressure relief openings.

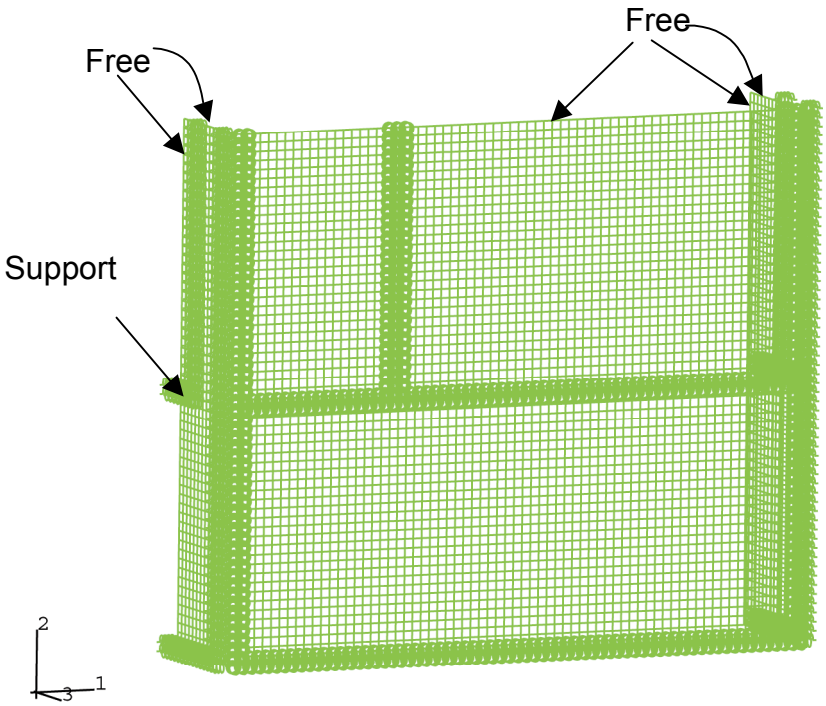

Figure 23. Finite element model.

The finite element model of the concrete structure is presented in Fig. 23. The FE model consists of nearly six thousand 4-noded double curved shell elements using reduced integration and hour glass control. The thickness of the wall is 0.6 m. Nine section points are used through the thickness. This wall is not designed to carry any pressure loads and its main purpose is to act as a radiation shield. There is vertical and horizontal reinforcement at the both faces of the wall. The amount of the reinforcement varies mainly between the minimum required and an amount of 0.27% of the cross section area of the wall.

In this study the connections to the surrounding structures were modelled as fully fixed. There is a structural seam between the containment and the reactor building. In order to simulate the effect of this seam, the upper edge and the vertical edges of the model were assumed to be free.
Damping was modelled by the mass proportional part of Rayleigh damping. Mass proportional damping was used to damp out the low frequency response. In this case, the mass proportional

damping was used for damping the lowest mode with 5.5 % of the critical damping. In simulating the structural behaviour during peak type detonation load, the effect of damping was almost negligible.

Material properties

Material non-linearities were simulated taking into account concrete cracking and strain rate dependent yield of the reinforcement.

Material properties for concrete are shown in Table 1. According to (RILEM Report 5 1991), high strain rate increases the tensile strength of concrete. Several theories have been developed in order to explain the strength increase due to high loading rates. Young's Modulus E_c is less affected by strain rate or even not affected at all. The tensile strength of concrete f_{ctk} was increased by approximating a higher tensile strength value for concrete according to the analytical and experimental results presented in (RILEM Report 5 1991). After cracking tensile stresses are assumed to decrease to zero when the corresponding strain is 0.0018. A cracked calculation point can only carry compressive stresses. Under tensile loading the crack naturally opens.

According to (RILEM Report 5 1991) high strain rates do not affect that strongly on compressive strength as on tensile strength. Compression crushing can not be taken into consideration in the ABAQUS/Explicit analyses. Compressive stresses were assumed to be linear. In evaluating the results, the compressive stresses in structure should be carefully studied. In considering these stresses, relatively high compressive stresses may locate on the surface of the wall. In this study compression crushing was assessed with an additional analysis using a modified Young's Modulus for concrete. This modulus is predicted using a compression crushing stress f_{ck} of 21 MPa and corresponding a strain of 3.5 $^{o}/_{oo}$.

Table 1. Concrete material properties.

E_c [MPa]	f_{ctk} [MPa]	υ	f_{cd} [MPa]	f_{ck} [MPa]
27000	3.0	0.15	15.6	21

The reinforcement was modelled by one-dimensional strain theory elements. Reinforcement was defined as layers of uniformly spaced reinforcing bars in the shell elements. Concrete cracking was considered independent of rebars. Effects between the concrete and the rebar interface, such as bond and dowel action, were approximately modelled by introducing some tension stiffening into the concrete cracking model. This simulated the load transfer across the cracks through the reinforcement.

The material behaviour of reinforcing steel was assumed to be linear elastic up to the yield stress. The stress vs. plastic strain is presented in Table 2. Young's modulus is 210 GPa and Poisson's ratio 0.3.

Table 2. Stress vs. plastic strain values for reinforcement steel.

Stress [MPa]	390	400	480	500
Plastic strain [mm/mm]	0	0.002	0.15	0.8

Yield stress of steel is strain rate dependent. In high strain rates the yield strength is higher than a normal static yield strength. This phenomenon essentially affects the results. The strain rate effect of reinforcing steel was accounted for by a standard procedure used for considering strain rate effects, and is expressed by the formula:

$$\dot{\bar{\varepsilon}}_{pl} = D\left[\frac{\tilde{\sigma}}{\sigma_y} - 1\right]^p \qquad (2)$$

where $\dot{\bar{\varepsilon}}$ is the equivalent plastic strain rate, $\tilde{\sigma}$ is the effective yield stress and σ_y is the static yield stress, (ABAQUS Theory Manual 1998). For structural steels these parameters are typically p = 5 and D = 40 (Bodner & Symonds 1979).

The effect of the strain rate dependence of the yield strength was studied and reported by Saarenheimo et al. (2001). According to Equation (2) the yield stress increases about 50 % when the strain rate reaches a value of 1/s.

Results

First a materially non-linear analysis was carried out in order to predict the ultimate capacity of the construction loaded with a constant pressure. In the following, the upper part on the right side of the structure (see Fig. 23) is considered. The upper edge is free and the distance between the supporting walls is 9.4 m. The reinforcement yielded at locations R9-R12 (see Fig. 27) at a pressure value of 0.1 MPa. In the field area the reinforcement starts to yield when the pressure value exceeds the value of 0.15 MPa. Compression crushing is remarkable at the supporting areas when the constant pressure is 0.2 MPa. At a pressure value of 0.2 MPa the inner surface in the field area near the upper free edge is crushed. The area between the supporting structures is called here as field area. Yielding in the reinforcement and crushing of the concrete occur widely when the constant pressure is further increased. The ultimate capacity of the wall, when considering the widest field area under constant pressure, is approximately slightly over 0.2 MPa.

Structural behaviour of the reinforced concrete wall was studied under detonation conditions corresponding to a detonable hydrogen mass of 3.15 kg. The calculation of loading transient is presented above. A special transfer tool was used for data transfer of pressure transients from the DET3D results to the ABAQUS/Explicit input (Silde and Pättikangas 2001). The peak type pressure loads are over in 30 ms. The overpressure after the peak detonation is assumed to decrease to zero in 0.25 seconds. The assumption is based on previous predictions presented by Saarenheimo (2000).

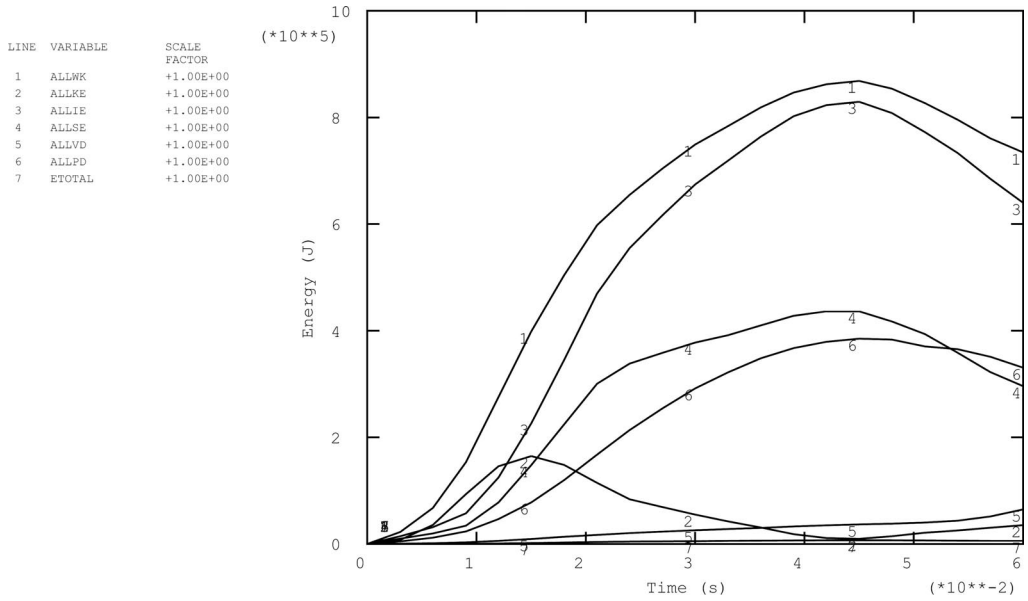

Figure 24. Energy balance during the first 60 ms.

The energy balance during 60 ms from the start of the detonation is shown in Fig. 24. The external work done by the pressure transients (ALLWK) creates the kinetic energy (ALLKE), the strain energy (ALLIE) and a part of the external work is dissipated by the viscous effects (ALLVD), like damping and strain rate dependent yield. Total strain energy consists further of recoverable strain energy (ALLSE) and the energy going to plastic deformations (ALLPD). During a rapid detonation simulation the effect of damping is negligible. ETOTAL shows the total energy balance (ETOTAL= ALLKE+ALLIE+ALLVD-ALLWK). The value ETOTAL is zero, if the energy balance holds.

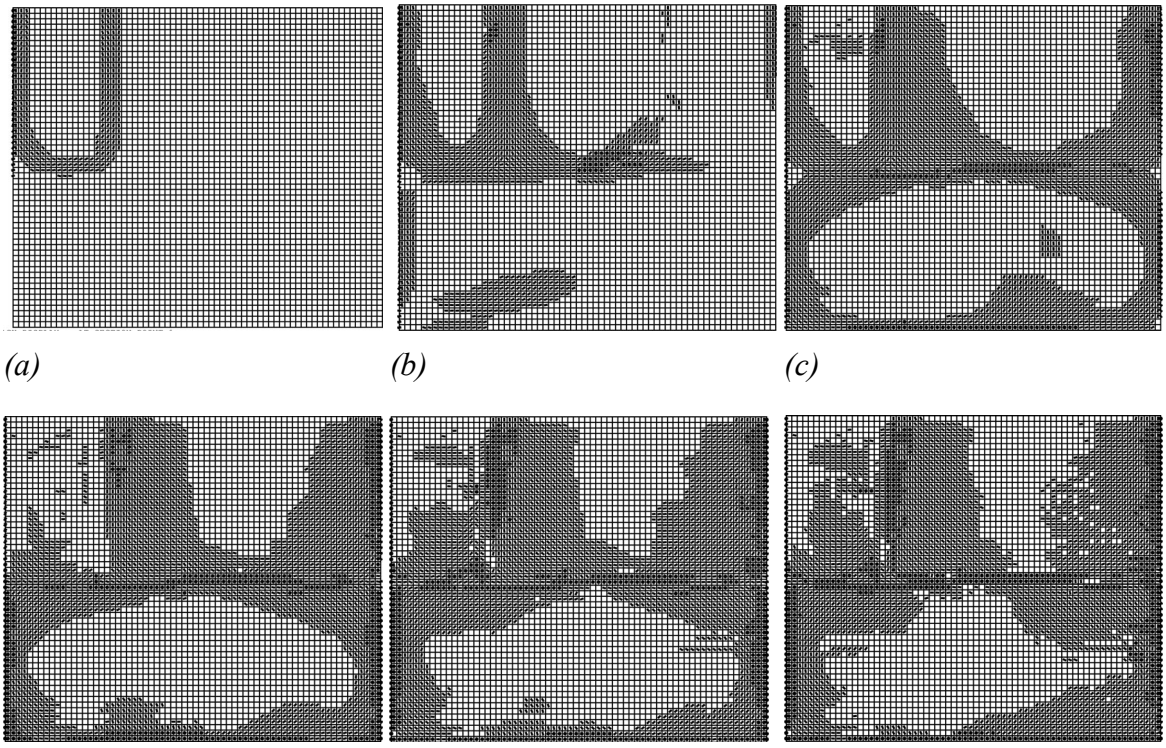

(a) *(b)* *(c)*

(d) *(e)* *(f)*

Figure 25 a-f. Open cracks on the inner surface of the wall, (a) t=3.0 ms, (b) t=7 ms and (c) t=14 ms. (d) t=20.0 ms, (e) t=30.0 ms and (f) t=60.0 ms.

Cracking on the inner surface of the structure corresponding different time increments t = 3 ms, 7 ms, 14 ms, 20 ms, 30 ms and 60 ms are presented in Fig. 25 a-f. Corresponding open cracks on the outer surface are presented in Fig. 26 a-f. It can easily be seen how the detonation starts near the upper left corner of the model and the pressure load travels on the inner surface of the structure. Cracking occurs firstly on the inner surface near the support areas and at the outer surface the cracking starts at the so called field areas.

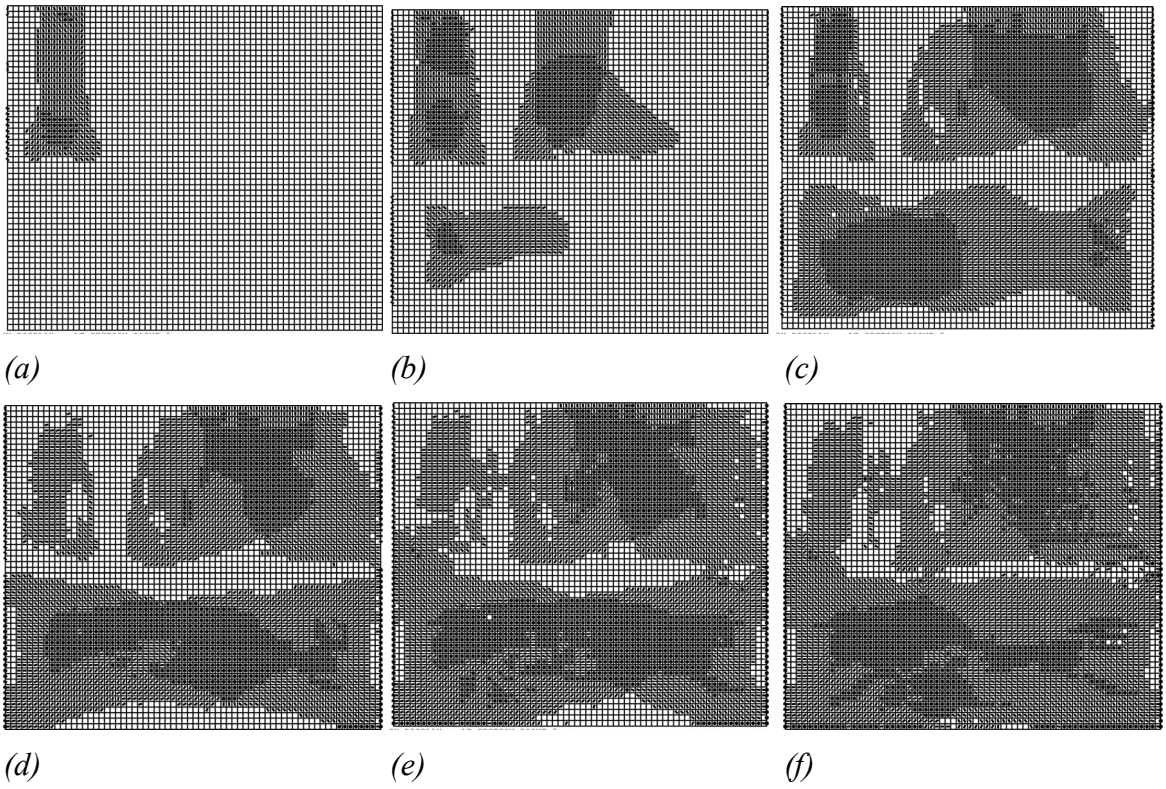

Figure 26 a-f. Open cracks on the outer surface of the wall, (a) t=3.0 ms, (b) t=7 ms and (c) t=14 ms. (d) t=20.0 ms, (e) t=30.0 ms and (f) t=60.0 ms.

Locations where stresses and strains in reinforcement are presented as a function of time, are shown in Fig. 27. Points referred to as R1, R2, R3 and R4 are located near the lower fixed edge of the model. Points R5-8 are located at level +25 m, where the connecting floor is modelled by boundary conditions. Points R9-12 are located near the right edge of the wall considered.

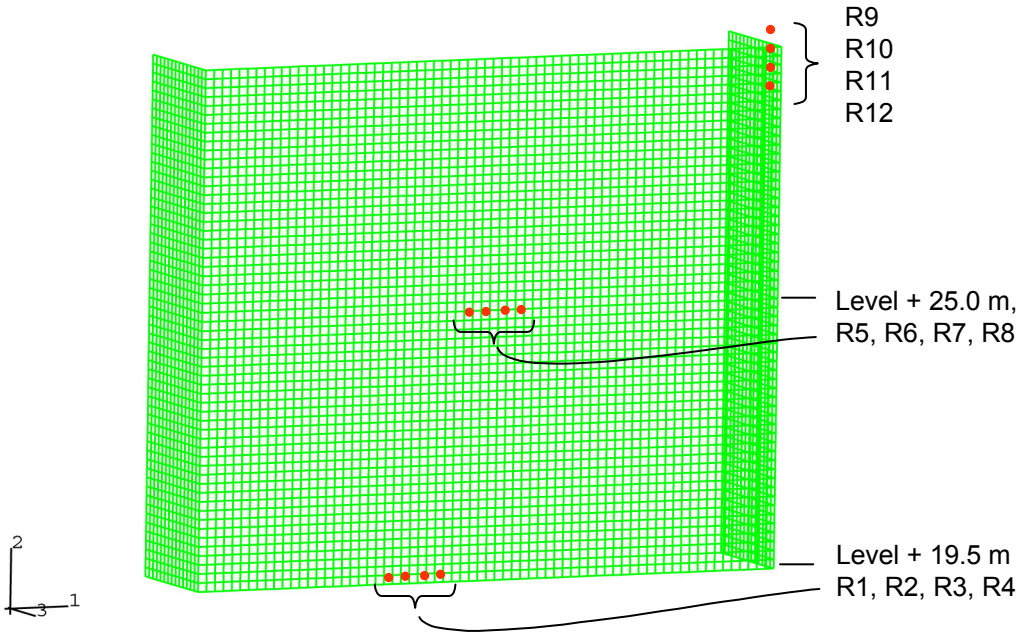

Figure 27. Locations for stress and strain output, Case A.

The inner vertical reinforcement is yielding near the horizontal supporting areas, at connecting floor levels +19.50 m and +25 m. Development of plastic deformation and stresses in the vertical reinforcement located at the inner surface of the wall, at locations R1-R4, is shown as a function of time in Fig 28 a and c, respectively. Corresponding results of plastic strain and stress in the vertical reinforcement located at the inner surface of the wall at locations R5-8 are presented in Fig. 28 b and d.

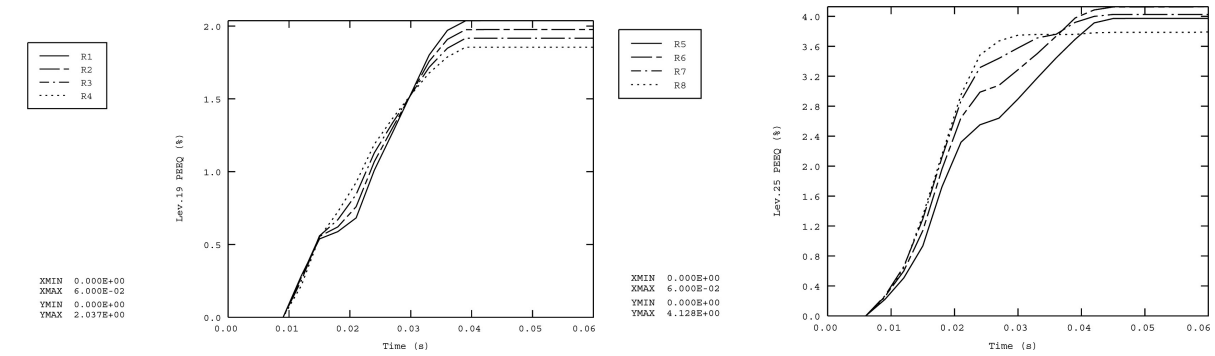

a) b)

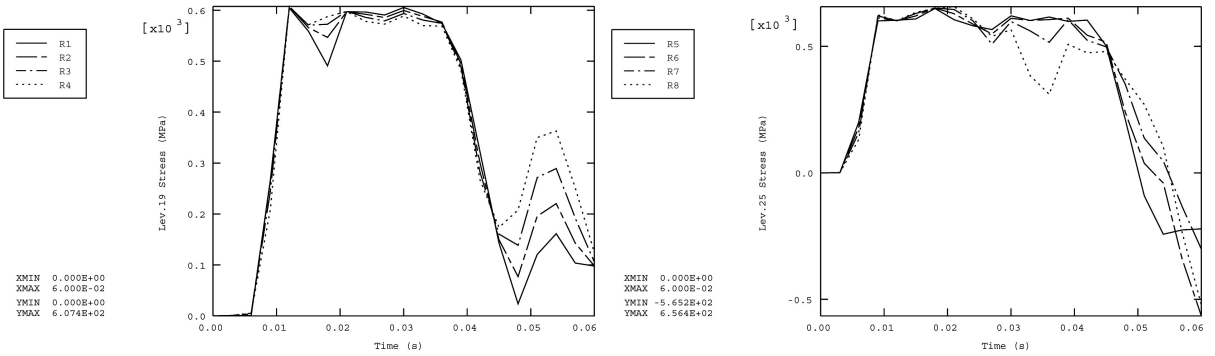

c) d)

Figure 28 a-d. (a) Plastic deformation as a function of time, R1-4, (b) plastic deformation as a function of time, R5-8. (c) Stress in reinforcement as a function of time, R1-4 and (d) Stress in reinforcement as a function of time, R5-8. Locations R1-8 are shown in Fig. 27.

As can be seen, the pressure load hits the location referred at R1-4 a couple of milliseconds later than it hits the location referred at R5-8 at level +25m.

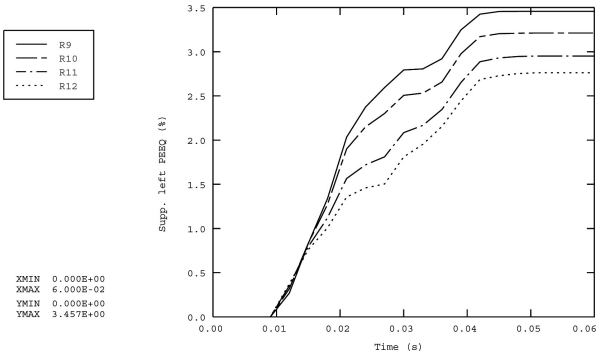

a)

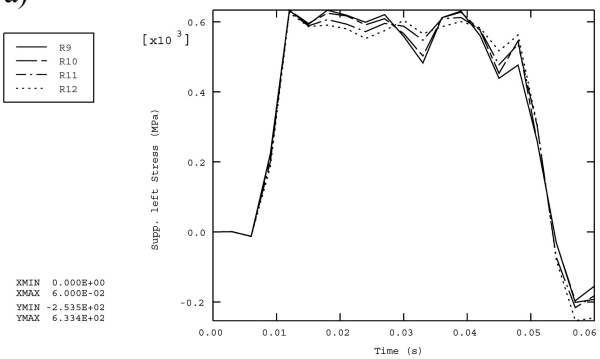

b)

Figure 29 a and b. (a) Plastic deformation as a function of time, R9-12, (b) Stress in reinforcement as a function of time, R9-12. Locations R9-R12 are shown in Fig. 27.

Remarkable yielding occurs near the right upper corner where the pressure transient hits the wall at t = 7 ms. Plastic strain and stress in reinforcement located at the inner surface of the wall near the right upper corner are shown in Fig, 29 a and b, respectively. At the end of the calculation, t = 60 ms, the maximum amount of plastic deformation is about 4% in the reinforcement located near the inner surface of the wall near the floor level +25 m and at the right upper corner. Vertical reinforcement located at the outer surface is yielding also, but the amount of plastic deformation is lower. This is because the detonation has just reached the right corner of the room. The plastic deformation in the vertical reinforcement located at the inner surface of the wall is less than 0.5 %. It should be noted that the results concerning reinforcement yielding were obtained without taking the compression crushing into consideration.

Compression crushing was predicted with a separate analysis using a reduced Young's modulus for the concrete. Minimum principal strains at t = 20 ms, 30 ms and 60 ms at the inner surface of the wall are shown in Fig. 30 a-c. Areas where compressive strains exceed the value of 3.5 $^{o}/_{oo}$ are indicated with red colour. In the field areas at the inner surface, compression crushing begins at the end of the detonation transient and continues during the slow pressure decrease after the peak detonations.

Minimum principal strains at t = 20 ms, 30 ms and 60 ms at the outer surface of the wall are shown in Fig. 31 a-c. Compression crushing begins at the outer surface near the support areas like connecting floors and walls already at t = 20 ms. The outer surface is widely compression crushed at t = 60 ms.

The ultimate capacity for a constant pressure was above estimated to be about 0.2 MPa for this kind of wall construction. The static type overpressure after the detonation peak is about 0.4 MPa and it is assumed to decrease to zero in 0.25 seconds. The lowest eigenfrequency of the wall is 27 Hz. The predicted time needed for the pressure decrease is relatively long compared with the lowest eigenperiod of the wall. So, this static type overpressure exceeds the capacity of the wall.

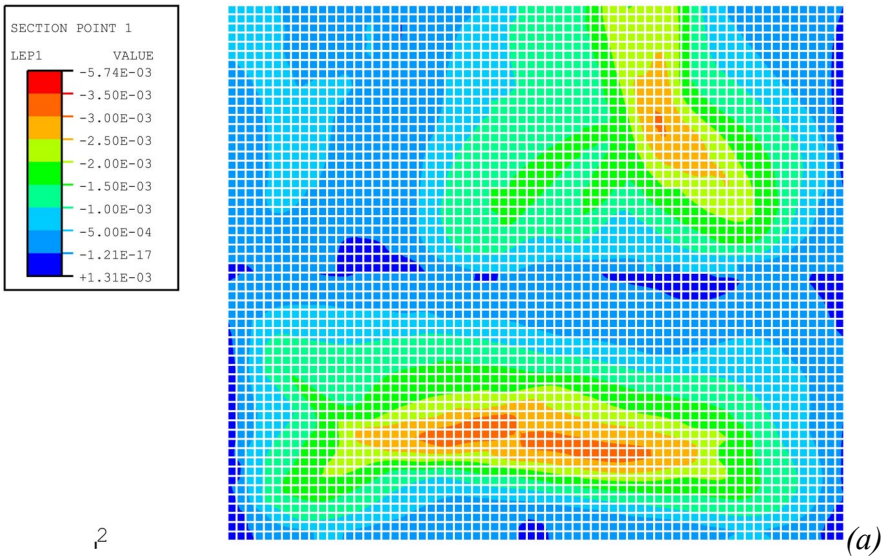

(a)

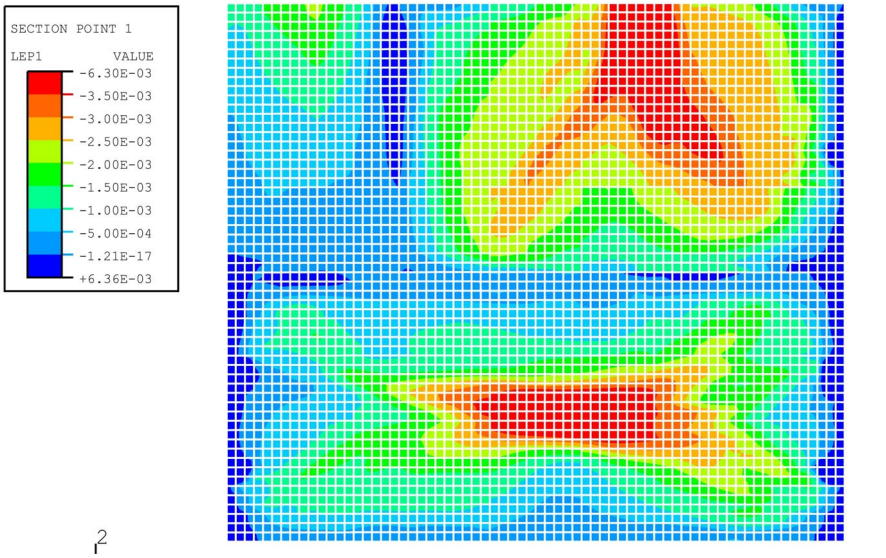

(b)

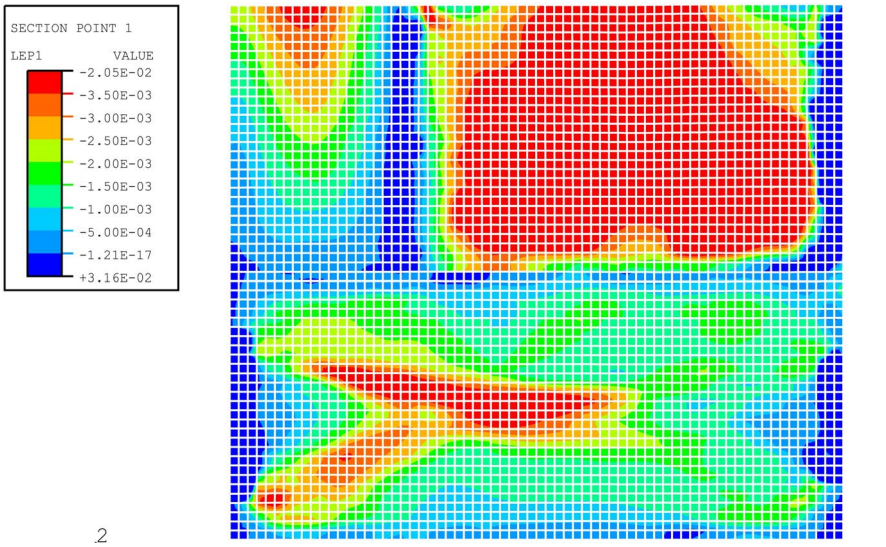

(c)

Figure 30 a-c. Minimum principal strain distribution at the inner surface, (a) t = 20 ms, (b) t = 30 ms and (c) t= 60 ms.

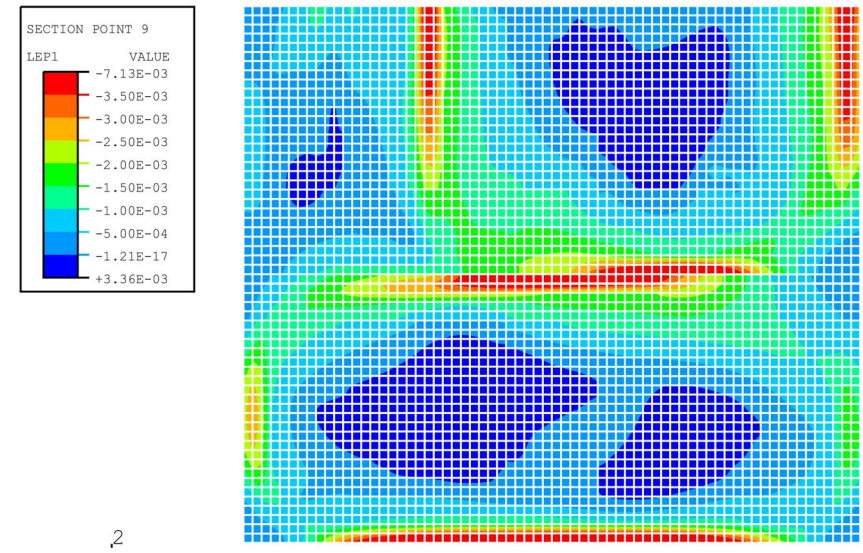

(a)

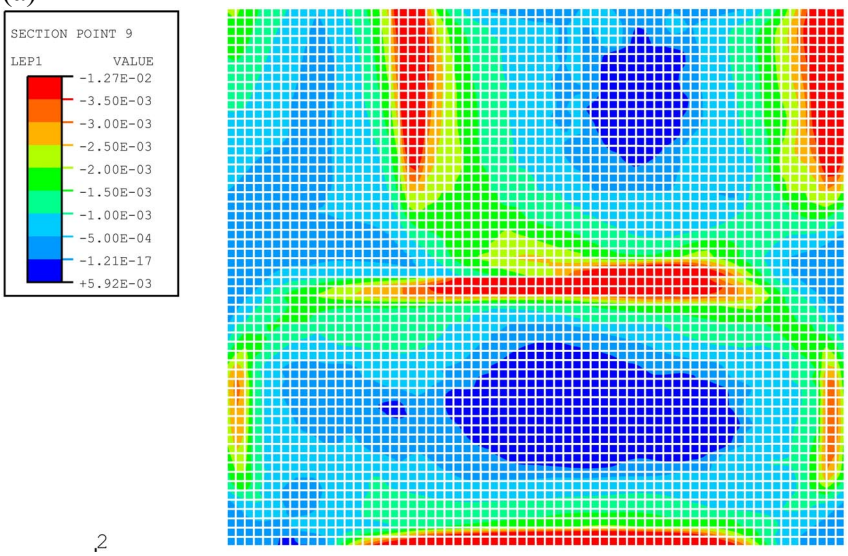

(b)

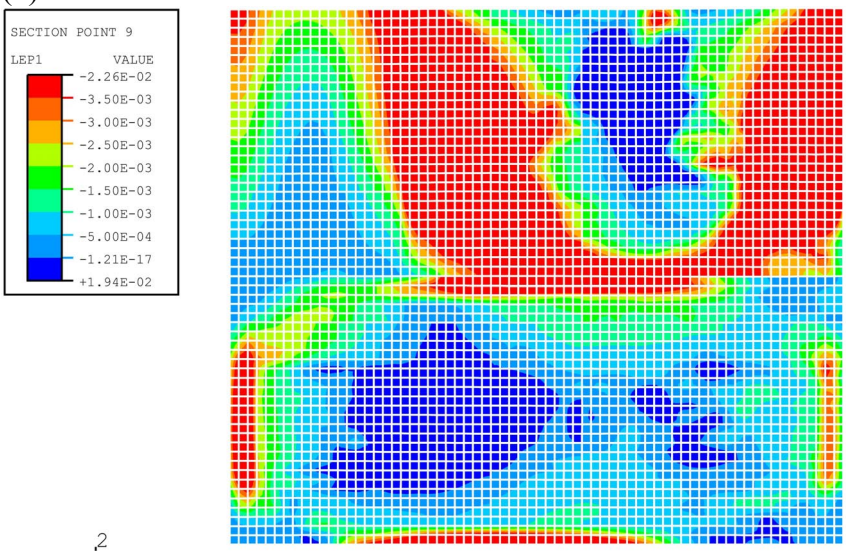

(c)

Figure 31 a-c. Minimum principal strain distribution at the outer surface. (a) t = 20 ms, (b) t = 30 ms and (c) t = 60 ms.

3.2 Pipe outlet

Structural integrity of a pipe outlet hit by the detonation wave was predicted using the ABAQUS/ Explicit code. In this study also the drag forces caused by the detonation transient were taken into consideration. The amount of detonable hydrogen was 3.15 kg and the detonation was assumed to occur at the same location as in the wall integrity considerations. Additional pressure transients due to the drag forces are presented in Figs 15-22. Pressure inside the pipe (the operating pressure) is 7.3 MPa.

Pipelines located in room B.60.80 are schematically shown in Fig. 5. Two pipelines leave horizontally from the containment wall at level + 26.0 m, make a 90-degree angle and continue vertically to the bottom of the room. In this study, the structural integrity of the pipe outlet located closer to the assumed detonation point is considered. A detail of the pipe outlet without insulation is shown in Fig. 32. There is a valve located between the pipe bend and the penetration to the containment wall. FE model used in these analyses and the main dimensions of the stainless steel AISI 304 pipe are shown in Fig. 33. The are 1950 four nodded shell elements and 11 600 degrees of freedom in the model. The mass of the valve and roughly the geometry of the valve were modelled.

The connection to the containment wall was assumed as fully fixed. The first pipe support can partly be seen in Fig. 32. The locations of the pipe supports are shown in Fig. 33 and they are referred as S1, S2 and S3 in the following. This steel structure supports both the horizontal part and the vertical part of the pipe bend. As can be seen in Fig. 32, the horizontal movements and displacement upward are restricted at the joint of the pipe bend and at the horizontal part of the pipe (S1). This same steel structure supports horizontally the pipe also just below the pipe bend, at the junction of the pipe bend and the vertical pipe line, at level + 24.8 m (S2). Because, only local behaviour of the pipe outlet is considered here, the pipe line is modelled until the next support which is located at level +19.6 m. This support, referred as S3, restricts only horizontal displacements. In this study the pipeline was thus not modelled completely. The stiffness of the pipe line outside this model naturally affects the results. In order to find out the effect of the boundary conditions at the end of the model (Fig. 33, support S3), this boundary condition was varied. Axial displacement was first assumed as free and then as fully fixed.

Figure 32. Pipe penetration in the containment

The gaps of the pipe supports are modelled with the non-linear spring elements. These spring elements are located at the nodes closest to the support. The number of spring elements simulating the contact is dependent of the width of the contacting support surface. At support S1 the contact is modelled at two nodes to each contacting global direction. Because the vertical global displacement is restricted only upwards, the number of spring elements is six. At support S2 there are three nodes along the pipe axis direction simulating the contact to each horizontal global direction, altogether there are twelve spring elements.

The support referred as S3 is modelled using only one spring element to simulate each horizontal gap. Gaps are modelled according to the design drawings and the size and corresponding global working directions of these gaps are listed in Table 3.

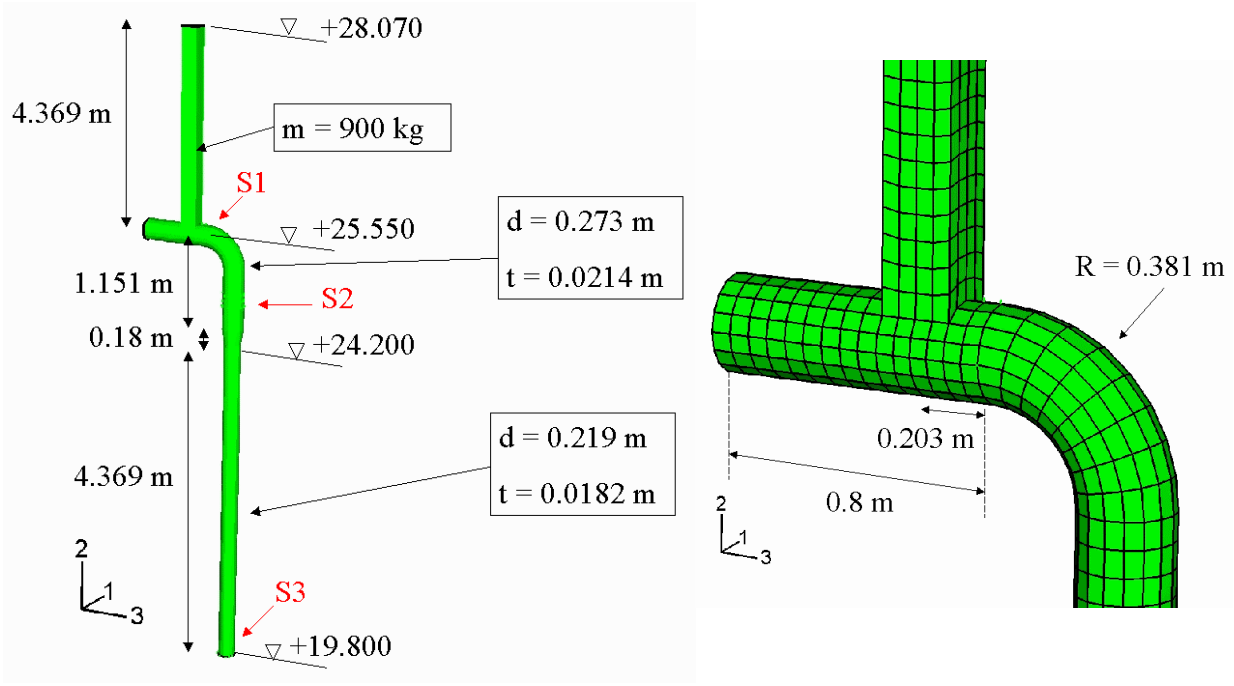

Figure 33. Main dimensions of the pipeline and a detail of FE model.

Table 3. Supports, gaps [mm].

Support	1-direction	2-direction	3-direction
S1 Level +25.55 m	+/- 3	+ 13	
S2 Level +24.8 m	+/- 4		+12/-4
S3 Level +19.8 m	+/-10		+/- 10

The pipe line is assumed to be in the operating temperature of 285°C and the operating pressure of 7,3 MPa. The pipeline was assumed to be filled with water. The mass of water was taken into account by effective density of the piping. The effect of damping was not considered in this study. The pressure transient due to the detonation load was used as loading (see Figs 9-22).

Piping steel

Both yield strength and ultimate tensile strength are diminished as the temperature increases. Material properties at the room temperature and operation temperature are given in Table 4, . Material properties used for the elastic-plastic material model are shown in Table 5 (Material Handboken 1994, Raaka-ainekäsikirja 1984).

Table 4. AISI304 material properties at the room temperature and operation temperature.

Temp. [°C]	Young's Modulus [GPa]	Yield Stress (0.2 %) [MPa]	Tensile Strength [MPa]	Thermal Expansion [1/°C]
25	201	210	515	1.7E-5
285	176	110	383	1.9E-5

Table 5. Stress vs. plastic strain values for piping steel AISI 304 at 285°C.

Stress [MPa]	100	110	120	383
Plastic strain [mm/mm]	0	0.002	0.01	0.4

Conservatively, the increase in yield strength properties at high strain rates was not considered here. According to Marshall et al. (1995), quasi static strength and toughness data appear to be conservative for stainless steels. According to IPIRG results increasing the strain rate by four orders of magnitude raised the yield strength significantly, but had only a modest effect on ultimate strength and fracture elongation at a temperature of 288°C. Also, the actual static yield strength is considerably higher than the corresponding yield strength provided by ASME Section III. The yield stress corresponding to a 0.2 % plastic strain was not measured in the IPIRG tests. The measured 2% offset yield strength at 288°C was 175 MPa, the corresponding value in ASME is 130 MPa. Measured yield stress corresponding to a 2 % strain at a strain rate of 1/s is about 200 MPa. Measured yield strength at strain rate of 10/s is 225 MPa.

Results

Structural analyses of a pipe outlet during the peak type detonation were carried out. In this study, also the drag forces were considered.
The development of plastic deformations at the outer surface of the pipe wall is shown in Fig. 34 a-d.

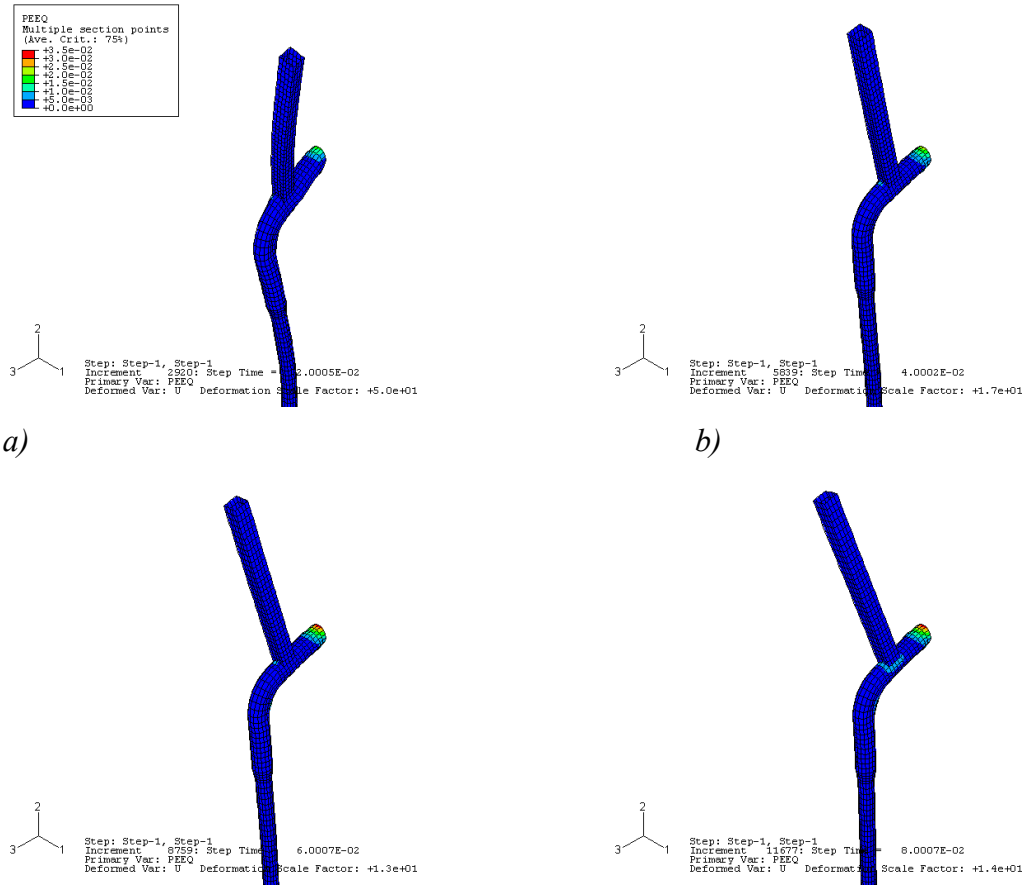

a) *b)*

c) *d)*

Figure 34 a-d. Deformed shape(scale factor varies) and equivalent plastic deformations due to a detonation loading (a) t = 30 ms, (b) t = 40 ms, (c) t = 60 ms and (d) t = 80 ms, lower end free. Areas, where the plastic deformation exceeds 3% are shown with red colour.

There are three spring elements above each other simulating the contact between the pipe wall and the support S2. These spring elements are referred here as follows: S2up means upper, S2m means middle and S2lo means the lowest spring element. During this simulation the pipe is at a continuous contact with the support to the negative 3-direction, see Fig. 35..

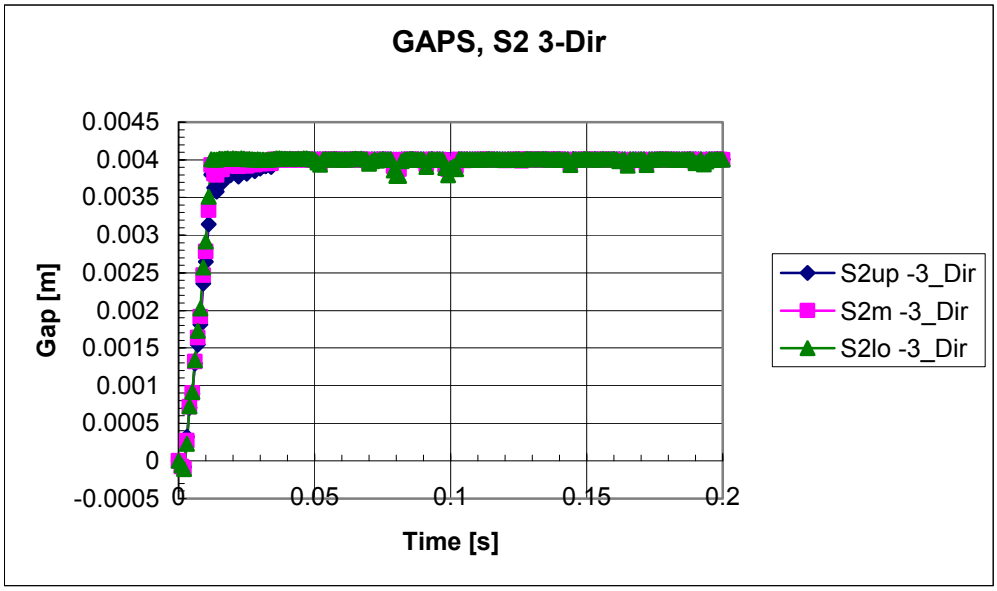

Figure 35. Contacts at support S2 to the negative 3-direction, free end.

The size of the gap in support S2 was 4 mm to the positive direction of 1-axis. This contact is presented as a function of time with blue line in Fig. 36. Contacts to the lower support S3 are presented also in Fig. 36. The pipe wall is modelled to the support, when the gap value is + 10 mm. The pipe almost lies on support S3 to the positive 3-direction. Contacts to the positive and negative global 1-directions at support S3 are presented with pink and green lines.

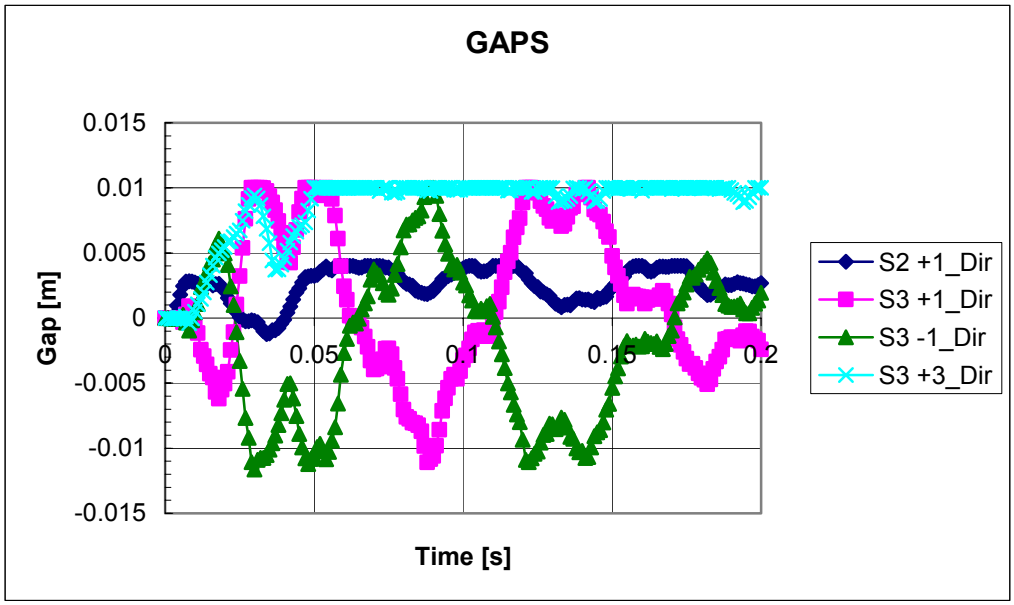

Figure 36. Contacts at support S2 to the positive 1-direction and at the support S3 to 1-direction and the positive 3-direction, fixed end.

The contact between the pipe wall and the suppports in the case where the axial displacements of the end of the pipe were assumed as zero are shown in Fig. 37. The pipe wall is now contacting to the support S2 in positive 1-direction at two nodal points (lower and middle). Also now there is an almost continuous contact between the pipe and the support S3 at the positive 3-direction.

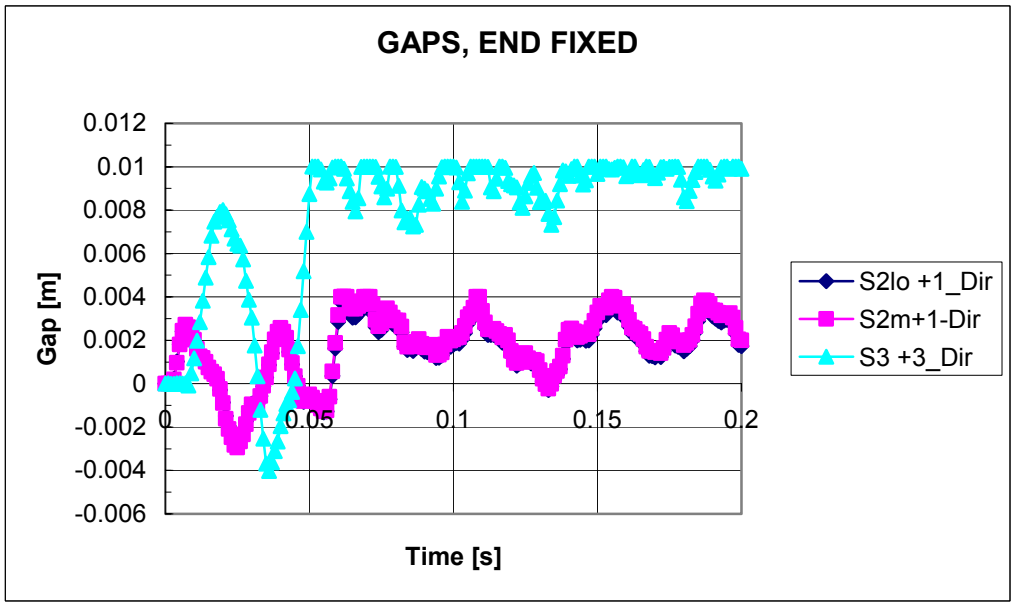

Figure 37. Contacts at supports S2 and S3, fixed end.

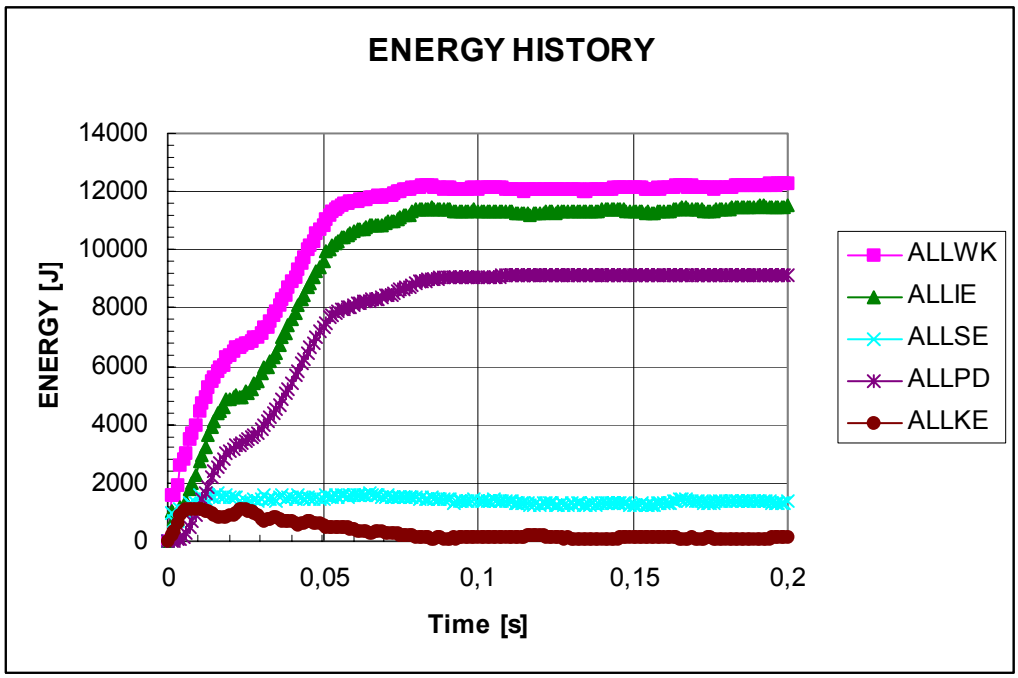

Figure38. Energy balance during the first 200 ms, free end.

The energy balance during 200 ms from the start of the detonation is shown in Fig. 38. Most of the energy goes to the plastic deformations.

If the axial displacement is assumed to be free at the lower end of the model, plastic deformations occur mainly near the penetration fixed to the reinforced concrete wall during the first 100 ms. As can be seen in Fig. 38, plastic energy is not increasing after t = 100 ms.

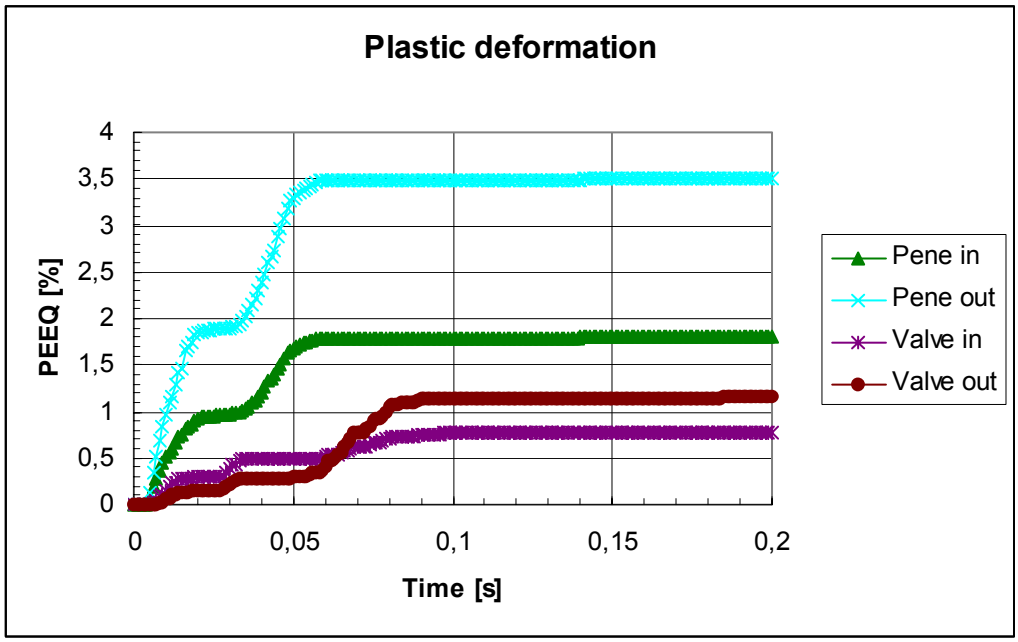

Figure 39. Plastic deformations at the inner and outer surfaces of the pipe wall near the wall penetration and near the valve connection.

Plastic deformations as a function of time near the penetration in two locations at the pipe wall are presented in Fig. 39. Maximum plastic deformation occurs at the outer surface of the pipe wall at the uppermost position, this is referred as 'Pene out'. The line referred as 'Pene in' shows the plastic deformation at the inner surface of the wall in the same location. Plastic deformations near the

junction of the valve are also shown at the outer and inner surfaces of the pipe wall. These curves are referred as 'Valve out' and 'Valve in'.

In the case where the lower end of the pipe is assumed to be fixed, the main plastic deformation occurs at the junction of the valve and the horizontal pipe line. The amount of plastic deformation near this junction is roughly the same in the both cases considered.

Drag forces mainly push the pipe line downwards and to the positive direction of the 1-axis. The highest drag forces are acting at the top of the valve to the positive 1-direction (see Fig. 16). This loading causes stresses mainly to the junction of the valve and the pipe. Especially, due to these dynamic impact forces hitting the top of the rather high valve, the effect of drag forces is remarkable considering the plastic deformations at the junction. Plastic deformations near the penetration to the containment wall are not increased due to the drag forces.

The calculation model in which the lower pipe end was assumed to move free axially, is a conservative model from the pipe penetration integrity point of view. Even in this conservative study, where damping or strain rate dependence of yield strength were ignored, the highest peak value for the maximum plastic deformation near the penetration through the containment wall is 3.5%. According to IPIRG tests the elongation at fracture is over 40 % and it is almost strain rate independent (Marschall & al. 1993).

According to Sammataro et al. (1993), the detail equivalent plastic strain in base metal or full penetration welds is limited to $0.80\varepsilon_u$, where ε_u is the ultimate strain in the base metal or weld metal, as applicable. The corresponding ultimate value for local equivalent plastic strain is $0.6\varepsilon_u$ for surface strain and $0.4\varepsilon_u$ for membrane strain. Corresponding values for free field equivalent plastic strain limits are $0.4\varepsilon_u$ and $0.25\varepsilon_u$. The maximum strain value according the calculation carried out using conservative boundary condition assumptions is 3.5% and it is well below these limit values.

4 Summary and Conclusions

Structural integrity of a reinforced concrete wall and a pipe penetration under detonation conditions in a selected reactor building room of Olkiluoto BWR were studied. Hydrogen leakage from the pressurised containment to the surrounding reactor building is possible during a severe accident. Leaked hydrogen tends to accumulate in the reactor building rooms where the leak is located leading to a stable stratification and locally very high hydrogen concentration. If ignited, a possibility to flame acceleration and detonation cannot be ruled out.

Detonation pressure loads were calculated with the DET3D code. Three-dimensional detonation simulations indicated that the highest pressure loads of about 7.0 MPa were reached near an upper corner of the analysed reactor building room. The highest pressure impulses on the wall during a 30 ms simulation were around 13 kPa-s.

The maximum pressure value simulated with DET3D just around the pipe penetration was approximately 1.8 MPa and occurred at $t \approx 2$ ms. After this instant of time, the pressure remained below 1.0 MPa, mostly around 0.5 MPa. The maximum pressure value around the pipeline was approximatively 1.5 MPa, except near the internal concrete floor at + 19.5 m, where the pressure peak was about 2 MPa.

Local gas velocities and related drag forces caused a significant pressure drop across the internal pipeline, especially above the level around + 25 m, where the detonation wave was allowed to propagate.

Materially non-linear dynamic analyses were carried out for the reinforced concrete wall with the ABAQUS Explicit code. Connecting structures like floors and walls were modelled as fully fixed. The strain rate dependence of yield strength of reinforcement was taken into consideration and this phenomenon affects the results considerably. In order to predict the compression crushing, structural analyses were carried out also using a reduced Young's modulus for the concrete.

The energy balance was maintained until the end of the calculation. In this case, plastic deformations occur mainly near the support areas. The amount of plastic deformation is less than 5 % due to the peak detonation loads during the first 30 ms of the detonation transient considered.

The structure may survive the peak detonation transient because the eigenperiod of the structure is considerably longer than the duration of the peak detonation. However, the relatively slowly decreasing static type pressure after a peak detonation damages the wall more severely. Elastic deformations in reinforcement are recoverable and cracks in these areas will close after the pressure decrease. But there will be remarkable compression crushing and the static type slowly decreasing over pressure clearly exceeds the loading capacity of the wall.

Structural integrity of a pipe outlet was considered also under detonation conditions. The effect of drag forces was taken into account. Damping and strain rate dependence of yield strength were not taken into consideration. The boundary condition at the end of the pipe line model was varied in order to find out the effect of the stiffness of the pipeline outside the calculation model. The calculation model where the lower pipe end is free to move axially, is conservative from the pipe penetration integrity point of view. Even in this conservative study, the highest peak value for the maximum plastic deformation is 3.5%. This is well below the success criteria found in literature.

5 References

ABAQUS Theory Manual. Version 5.8 1998. Hibbit, Karlsson & Sorensen Inc. Rhode Island (RI).

ABAQUS/Explicit Lectures. 1996. Analysis of Concrete Structures Using ABAQUS/Explicit. 1996.

Breitung, W. and Redlinger, R. 1994. Containment Loads from Hydrogen Detonations in Severe Accidents, Kerntechnik 59(1994) pp 162-170.

Bodner S. R. & Symonds P. S. 1979. Experiments on Viscoplastic Response of Circular Plates to Impulsive Loading. Journal of Mechanics and Physics of Solids. pp 91-119.

Kinney, G. F., and Graham, K. J. 1985. Explosive Shocks in Air. Springer-Verlag. 1985.

Manninen, M., Huhtanen, R., Lindholm, I., and Sjövall, H. 2000. Hydrogen in BWR Reactor Building. Proceedings of ICONE 8, 8th International Conference on Nuclear Engineering, April 2-6, 2000, Baltimore, MD, USA.

Manninen, M., Silde, A., Lindholm, I., Huhtanen, R. and Sjövall, H. 2002.
Simulation of Hydrogen Deflagration and Detonation in a BWR Reactor Building.
Nuclear Engineering and Design 211 (2002) 27 - 50.

Marschall, C. W., Landow, M. P., Wilkowski, G. M. 1993. Loading Rate Effects on Strength and Fracture Toughness of Pipe Steels Used in Task 1 of the IPIRG Program. NRCNUREG7CR-6098.

Marschall, C. W., Landow, M. P., Wilkowski, G. M. and Rosenfield, A. R. 1995. Comparison of Static and Dynamic Strength and J-R Curves of Various Piping Materials from the IPRG-1 Program. Int. J. Pres. Ves. & Piping 62 (1995) pp. 49-58.

Materialhandboken, Kapitel 1. 1994. Normer och datablad för metalliska material. ABB Atom Västeros 1994.

Raaka-ainekäsikirja. 1984. Valmet Oy Rautpohja. Satapaino, Tampere 1984.

RILEM REPORT 5.1991 Fracture Mechanics Test Methods for Concrete. Edited by Shah S.P. and Carpinteri A. Chapman and Hall London-New York Tokyo Melbourne Madras 1991. 287 p.

Saarenheimo, A., Hyvärinen, J. 1996. Finite Element Analysis of a Steel Containment under Detonation Conditions. Presented at the SUSI 96 Conference (Structures Under Shock and Impact) held in Udine, Italy, 3-5 July, 1996.

Saarenheimo, A. 2000. Reinforced Concrete Wall under Hydrogen Detonation. Roskilde: NKS. 45 p. Report NKS-26. ISBN 87-7893-077-4.

Sammataro, R. F., Solonick, W. R. & Edwards, N. W., 1993. A Generic Approach for Steel Containment Vessel Success Criteria for Severe Accident Loads. Nucl. Eng. and Design 145 (1993) pp. 289-305.

Silde, A. and Pättikangas, T. 2001. D2A Version 1.0: Interface between the DET3D and ABAQUS Codes. Programme Document ENE4-PD-3/01. VTT Energy.

Silde, A. & Lindholm, I. 2000. On Detonation Dynamics in Hydrogen-Air-Steam Mixtures: Theory and Application to Olkiluoto Reactor Building. Roskilde: NKS. 83 p. Report NKS-9. ISBN 87-7893-058-8.

Silde, A. and Redlinger, R. 2001. Three Dimensional Simulation of Hydrogen Detonations in the Olkiluoto BWR Reactor Building. NKS report NKS-27, ISBN 87-7893-078-2.

Zel'dovich, Ya. B., and Raizer, Yu.P. 1996. Physics of Shock Waves and High-Temperature Hydrodynamic Phenomena. Academic Press. 1966

Bibliographic Data Sheet **NKS-73**

Title	Structural integrity of a reinforced concrete structure and a pipe outlet under hydrogen detonation conditions
Author(s)	Arja Saarenheimo, Ari Silde & Kim Calonius
Affiliation(s)	VTT Industrial Systems, Finland
ISBN	87-7893-129-0
Date	May 2002
Project	NKS/SOS-2.3
No. of pages	40
No. of tables	5
No. of illustrations	39
No. of references	19

Abstract

Structural integrity of a reinforced concrete wall and a pipe penetration under detonation conditions in a selected reactor building room of Olkiluoto BWR were studied. Hydrogen leakage from the pressurised containment to the surrounding reactor building is possible during a severe accident. Leaked hydrogen tends to accumulate in the reactor building rooms where the leak is located leading to a stable stratification and locally very high hydrogen concentration. If ignited, a possibility to flame acceleration and detonation cannot be ruled out.

The structure may survive the peak detonation transient because the eigenperiod of the structure is considerably longer than the duration of the peak detonation. However, the relatively slowly decreasing static type pressure after a peak detonation damages the wall more severely. Elastic deformations in reinforcement are recoverable and cracks in these areas will close after the pressure decrease. But there will be remarkable compression crushing and the static type slowly decreasing over pressure clearly exceeds the loading capacity of the wall.

Structural integrity of a pipe outlet was considered also under detonation conditions. The effect of drag forces was taken into account. Damping and strain rate dependence of yield strength were not taken into consideration. The boundary condition at the end of the pipe line model was varied in order to find out the effect of the stiffness of the pipeline outside the calculation model. The calculation model where the lower pipe end is free to move axially, is conservative from the pipe penetration integrity point of view. Even in this conservative study, the highest peak value for the maximum plastic deformation is 3.5%. This is well below the success criteria found in literature.

Key words

Non-linear reinforced concrete, pipe outlet, hydrogen detonation, finite element analysis

Available on request from the NKS Secretariat, P.O.Box 30, DK-4000 Roskilde, Denmark.
Phone (+45) 4677 4045, fax (+45) 4677 4046, e-mail nks@catscience.dk, www.nks.org.